An Extreme Case of Swelling of Mostly-c*is* Polydicyclopentadiene by Selective Solvent Absorption - Application in Decontamination and Environmental Remediation

*Despoina Chriti, Grigorios Raptopoulos, George C. Anyfantis, Patrina Paraskevopoulou**

Laboratory of Inorganic Chemistry, Department of Chemistry, National and Kapodistrian University of Athens, Panepistimiopolis Zografou, Athens 15771, Greece

*E-mail: paraskevopoulou@chem.uoa.gr

SUPPORTING INFORMATION

Table of Contents

Figure S1. FTIR-ATR spectrum of **W_2-PDCPD** xerogels. **6**

Figure S2. . ^{13}C CPMAS NMR spectrum of **W_2-PDCPD** xerogels. **6**

Figure S3. Differential thermogravimetric analysis of **W_2-PDCPD** xerogels. **7**

Figure S4. Swelling of a **W_2-PDCPD** xerogel in chloroform with time. **8**

Figure S5. Swelling of a **W_2-PDCPD** xerogel in bromobenzene with time. **8**

Figure S6. Swelling of a **W_2-PDCPD** xerogel in carbon disulfide with time. **9**

Figure S7. Swelling of a **W_2-PDCPD** xerogel in 1,3-dichlorobenzene with time. **9**

Figure S8. Swelling of a **W_2-PDCPD** xerogel in carbon tetrachloride with time. **10**

Figure S9. Swelling of a **W_2-PDCPD** xerogel in chlorobenzene with time. **10**

Figure S10. Swelling of a **W_2-PDCPD** xerogel in 1,2-dibromoethane with time. **11**

Figure S11. Swelling of a **W_2-PDCPD** xerogel in tetrahydrofuran with time. **11**

Figure S12. Swelling of a **W_2-PDCPD** xerogel in benzene with time. **12**

Figure S13. Swelling of a **W_2-PDCPD** xerogel in ethyl bromide with time. **12**

Figure S14. Swelling of a **W_2-PDCPD** xerogel in 1-bromobutane with time. **13**

Figure S15. Swelling of a **W_2-PDCPD** xerogel in methylene dichloride with time. **13**

Figure S16. Swelling of a **W_2-PDCPD** xerogel in 1,3,5-trimethylbenzene with time. **14**

Figure S17. Swelling of a **W_2-PDCPD** xerogel in 1,4-dimethylbenzene with time. **14**

Figure S18. Swelling of a **W_2-PDCPD** xerogel in 1,3-dimethylbenzene with time. **15**

Figure S19. Swelling of a **W_2-PDCPD** xerogel in 1,2-dichlorobenzene with time. **15**

Figure S20. Swelling of a **W_2-PDCPD** xerogel in benzyl chloride with time. **16**

Figure S21. Swelling of a **W_2-PDCPD** xerogel in cyclohexane with time. **16**

Figure S22. Swelling of a **W_2-PDCPD** xerogel in 1,4-dioxane with time. **17**

Figure S23. Swelling of a **W_2-PDCPD** xerogel in cyclohexanone with time. **17**

Figure S24. Swelling of a **W_2-PDCPD** xerogel in 1,2-dichloroethane with time. **18**

Figure S25. Swelling of a **W_2-PDCPD** xerogel in pyridine with time. **18**

Figure S26. Swelling of a **W_2-PDCPD** xerogel in bromobenzene. **19**

Figure S27. Swelling of a **W_2-PDCPD** xerogel in carbon disulfide. **19**

Figure S28. Swelling of a **W_2-PDCPD** xerogel in 1,2-dibromoethane. **19**

Figure S29. Swelling of a **W_2-PDCPD** xerogel in 1,3,5-trimethylbenzene. **20**

Figure S30. Swelling of a **W_2-PDCPD** xerogel in 1,4-dimethylbenzene. **20**

Figure S31. Swelling of a **W_2-PDCPD** xerogel in 1,3-dimethylbenzene. **20**

Figure S32. Swelling of a **W_2-PDCPD** xerogel in benzyl chloride. **21**

Figure S33. Swelling of a **W_2-PDCPD** xerogel in 1,4-dioxane. **21**

Figure S34. Relation between the experimental maximum volume degree of swelling (q_{max}) of **W_2-PDCPD** xerogels and the Hansen Solubility Parameters (HSP): total solubility parameter (δ_T, a), D-component (δ_D, b), P-component (δ_P, c) and H-component (δ_H, d) of the respective solvents. **25**

Figure S35. 3D plot of the individual Hansen Solubility Parameters (HSP) for each solvent tested. Blue dots represent solvents in which **W_2-PDCPD** xerogels swelled (23 "good" solvents – score: "1"). Red squares represent solvents in which no swelling was observed (21 "bad" solvents – score: "0"). The green sphere, generated by the HSPiP 5.1.02 software, is the sphere with the minimum diameter that fits best the experimental data. The center of the sphere is a reasonable estimate of the HSP of **W_2-PDCPD**, which is represented by the green dot. The sphere contains all "good" solvents and no "bad" solvents (referred to as wrong solvents), giving a fit value of 1.0, which is considered as a perfect fit. **28**

Figure S36. 2D projections, generated by the HSPiP 5.1.02 software, of the individual Hansen Solubility Parameters (HSP) for each solvent tested at the three planes of the cube inscribing the sphere of Figure S35, as indicated. Blue dots represent solvents in which **W_2-PDCPD** xerogels swelled ("good" solvents). Red squares represent solvents in which no swelling was observed ("bad" solvents). The green dot represents **W_2-PDCPD** itself. The green circle contains all "good" solvents. **28**

Figure S37. 2D projections, generated by the HSPiP 5.1.02 software, of the individual Hansen Solubility Parameters (HSP) for each solvent tested at the three planes of the cube inscribing the

sphere of Figure 5 of the manuscript, as indicated. Blue dots represent solvents in which **W_2-PDCPD** xerogels swelled ("good" solvents). Red squares represent solvents in which no swelling was observed ("bad" solvents). The green dot represents **W_2-PDCPD** itself. The green circle contains all "good" solvents. **29**

Figure S38. Calculation of the Hansen Solubility Parameters (HSP) of dicyclopentadiene (DCPD) using the DIY method of the HSPiP 5.1.02 software. **29**

Figure S39. Same as Figure 5 of the manuscript, showing also the location of dicyclopentadiene (DCPD; orange dot; RED = 0.438). **30**

Figure S40. 2D plots of the magnitude differences between the solvent and **W_2-PDCPD** xerogels: $\Delta\delta_P$ *vs* $\Delta 2\delta_D$ (a) and $\Delta\delta_H$ *vs* $\Delta 2\delta_D$ (b). Green dot shows point (0,0). **32**

Figure S41. Separation of methylene dichloride (dyed with Sudan blue) from water using **W_2-PDCPD** xerogels. **33**

Figure S42. Separation of chlorobenzene (dyed with Sudan blue) from water using **W_2-PDCPD** xerogels. **33**

Figure S43. Separation of 1,3-dichlorobenzene (dyed with Sudan blue) from water using **W_2-PDCPD** xerogels. **33**

Figure S44. Separation of benzyl chloride (dyed with Sudan blue) from water using **W_2-PDCPD** xerogels. **34**

Figure S45. Separation of tetrahydrofuran from water using **W_2-PDCPD** xerogels. **34**

Figure S46. Separation of toluene from oil using **W_2-PDCPD** xerogels. **34**

Figure S47. Separation of toluene from hexane using **W_2-PDCPD** xerogels. **35**

Table S1. Solvent uptake and density of **W2-PDCPD** xerogels and other materials from the literature, for comparison purposes. **23**

Table S2. Experimental maximum volume degree of swelling (q_{max}) of **W2-PDCPD** xerogels in various solvents; Hansen Solubility Parameters (HSP),[24] molar volume (V_m)[24] and surface tension (γ) of the solvents used in this study. **24**

Table S3. Experimental maximum volume degree of swelling (q_{max}) of **W2-PDCPD** xerogels in various solvents, Hansen Solubility Parameters (HSP) of the solvents,[24] scoring according to whether they are "good" ("1") or "bad" ("0") solvents, and calculated Relative Energy Differences (RED). **27**

Table S4. Calculated Hansen Solubility Parameters (HSP) of **W2-PDCPD** xerogels and solvents. **31**

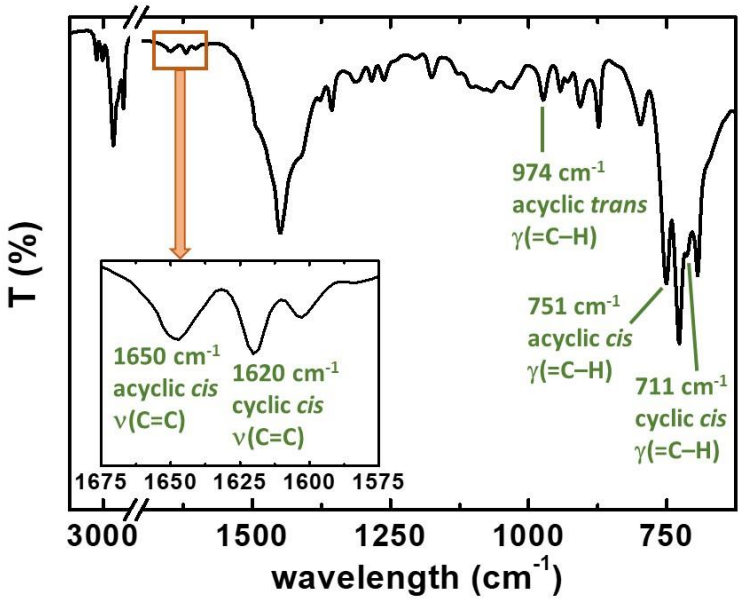

Figure S1. FTIR-ATR spectrum of **W_2-PDCPD** xerogels.

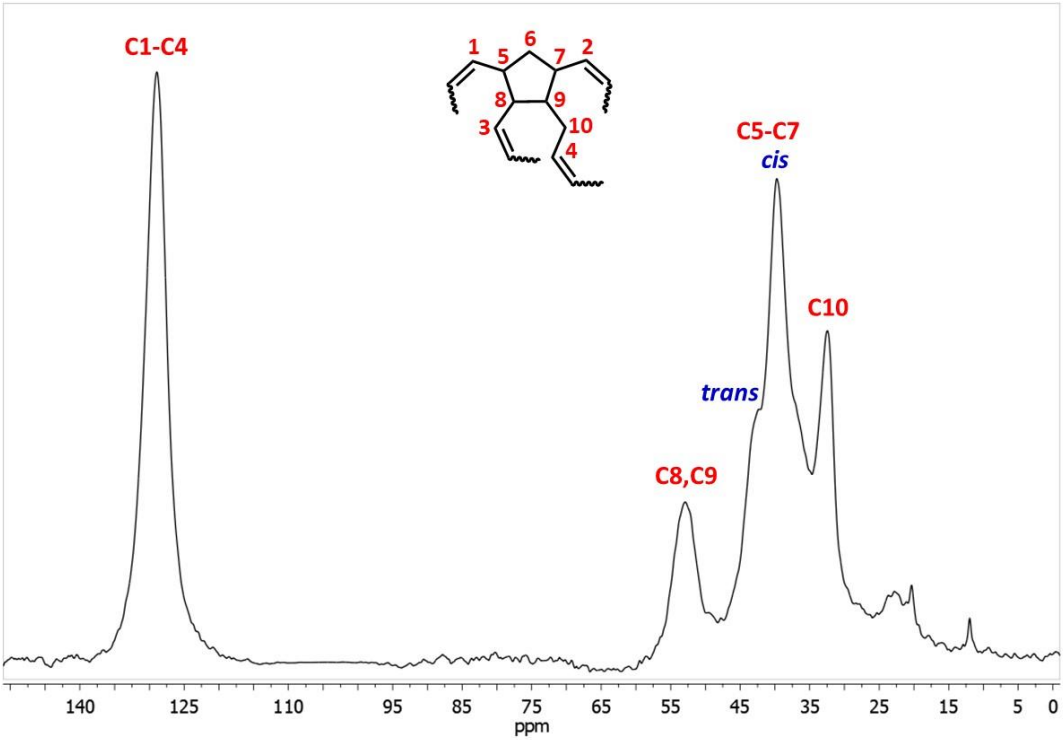

Figure S2. . ^{13}C CPMAS NMR spectrum of **W_2-PDCPD** xerogels.

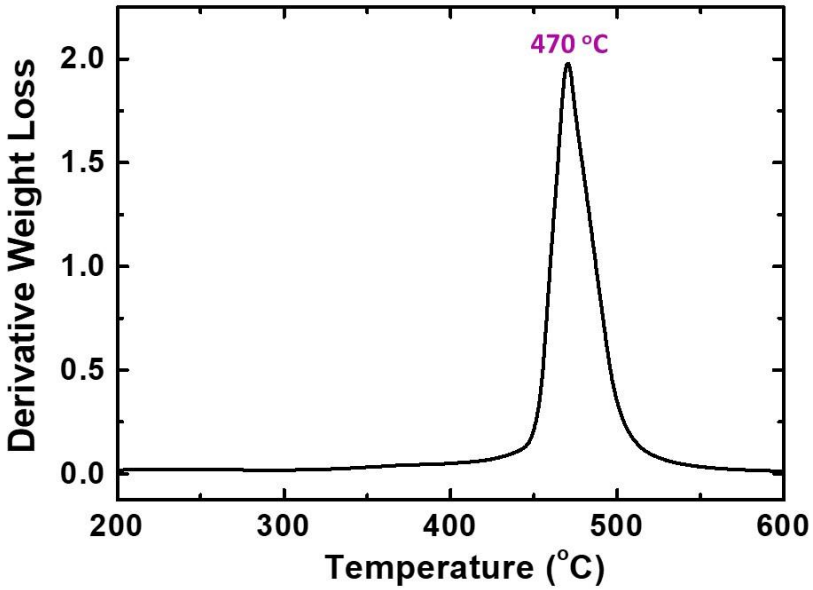

Figure S3. Differential thermogravimetric analysis of **W_2-PDCPD** xerogels.

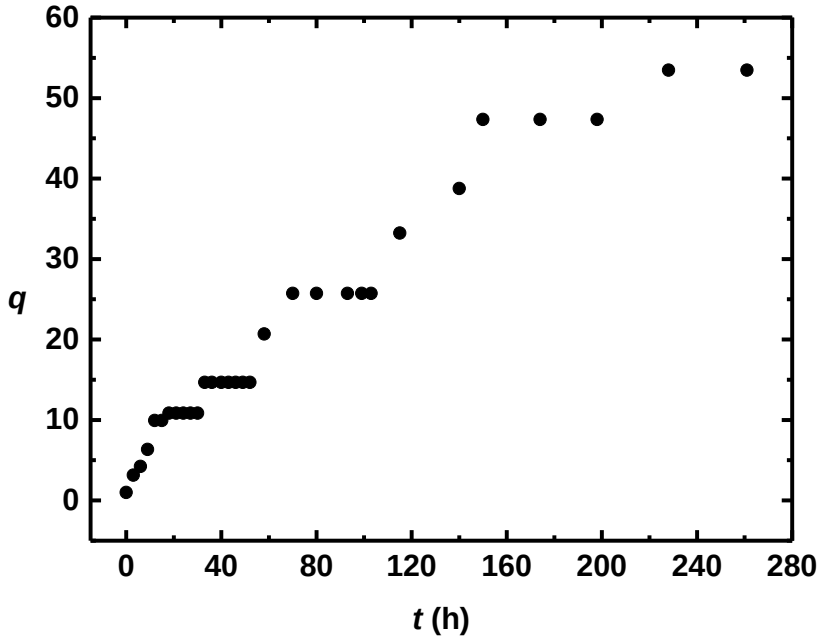

Figure S4. Swelling of a **W_2-PDCPD** xerogel in chloroform with time.

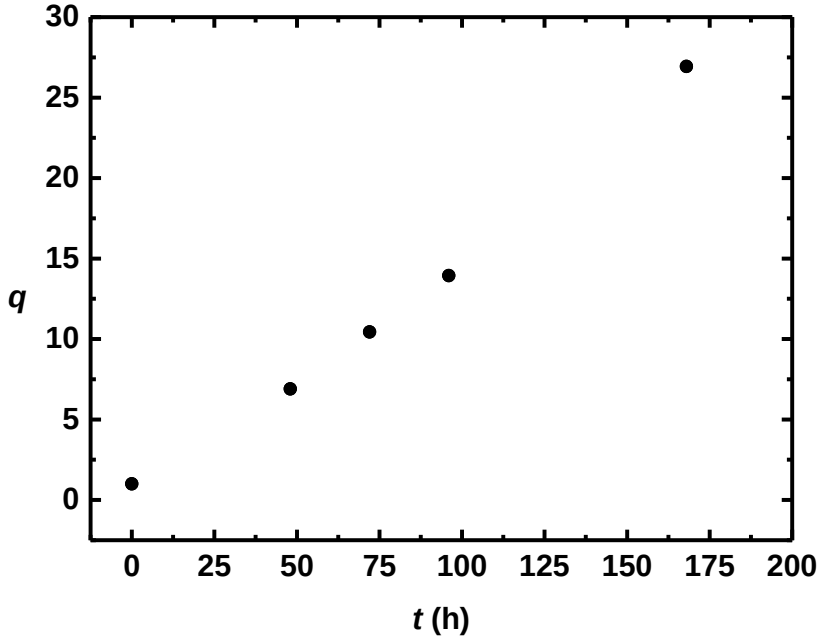

Figure S5. Swelling of a **W_2-PDCPD** xerogel in bromobenzene with time.

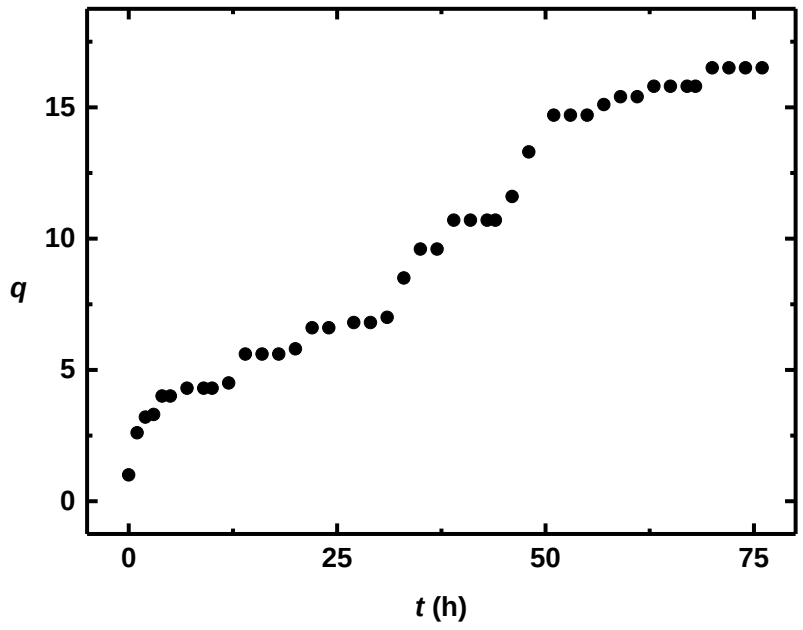

Figure S6. Swelling of a **W_2-PDCPD** xerogel in carbon disulfide with time.

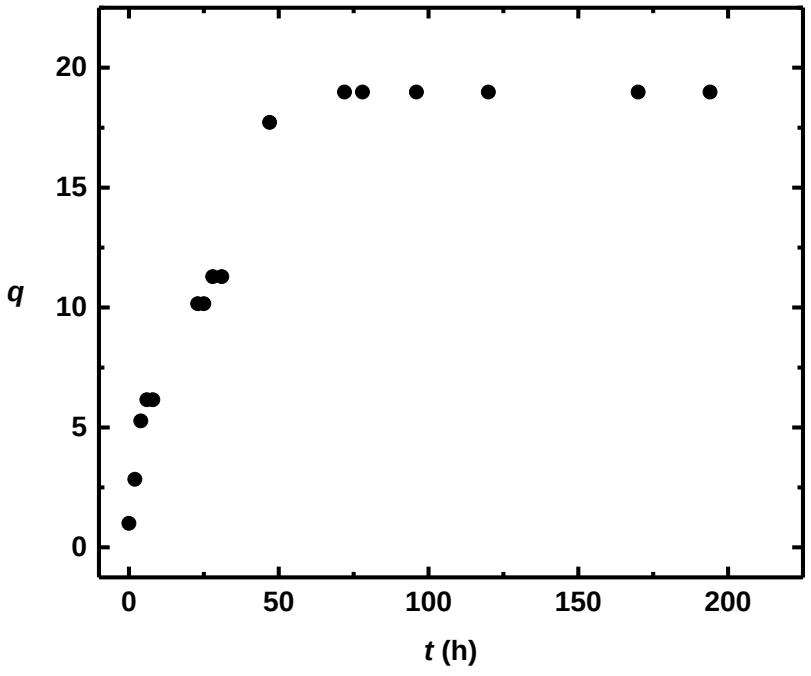

Figure S7. Swelling of a **W_2-PDCPD** xerogel in 1,3-dichlorobenzene with time.

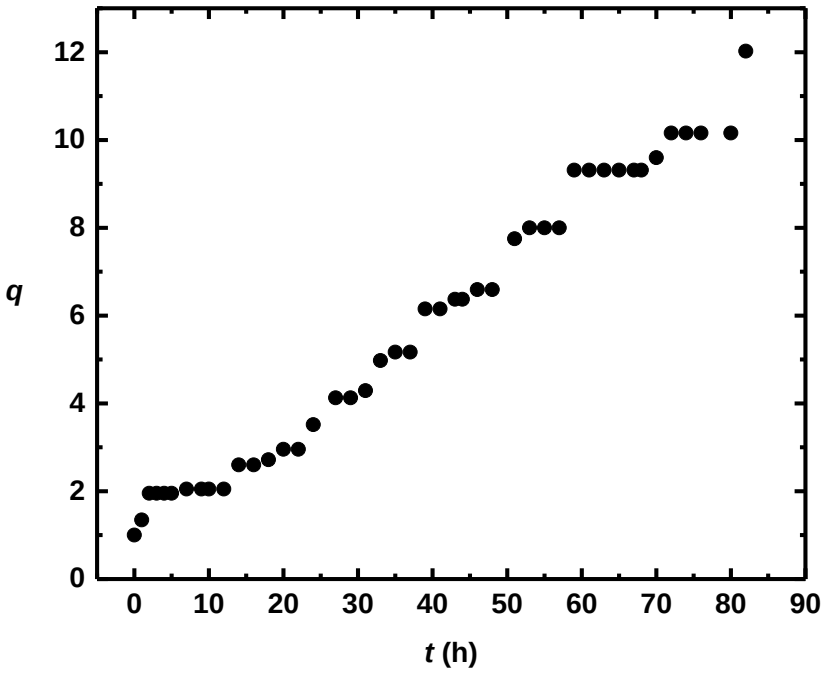

Figure S8. Swelling of a **W_2-PDCPD** xerogel in carbon tetrachloride with time.

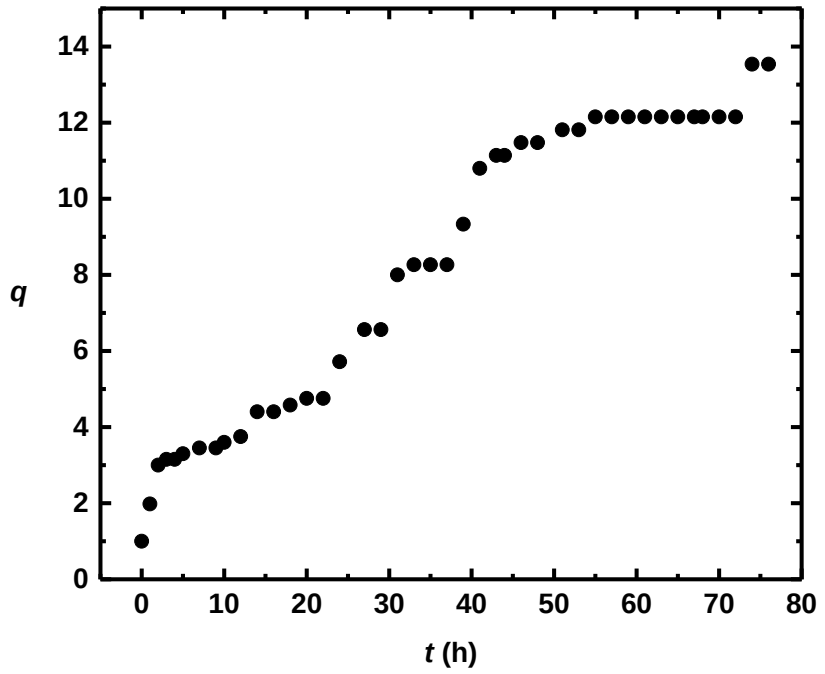

Figure S9. Swelling of a **W_2-PDCPD** xerogel in chlorobenzene with time.

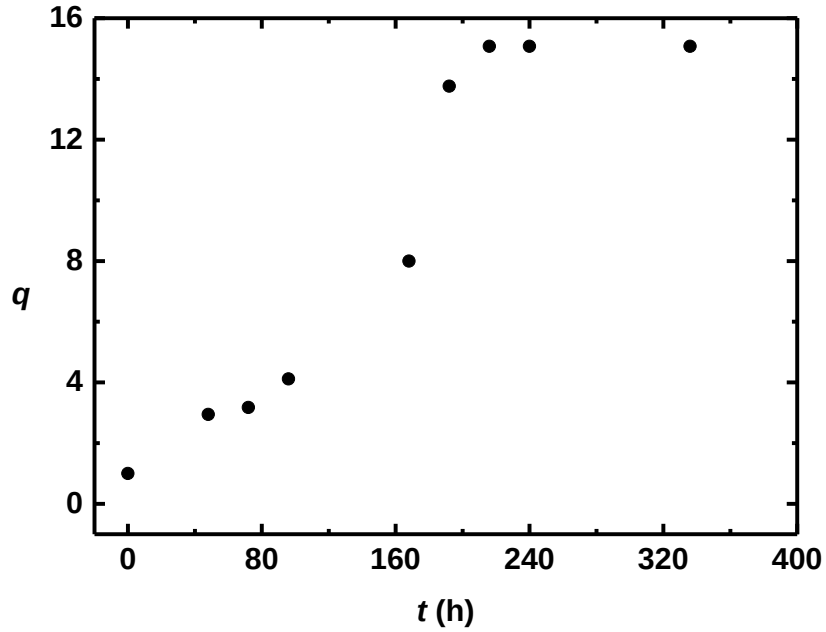

Figure S10. Swelling of a **W_2-PDCPD** xerogel in 1,2-dibromoethane with time.

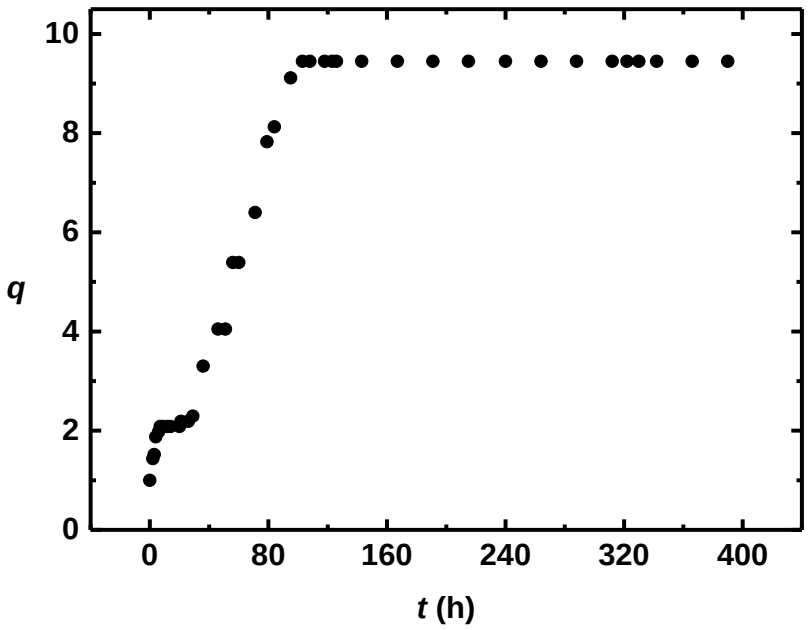

Figure S11. Swelling of a **W_2-PDCPD** xerogel in tetrahydrofuran with time.

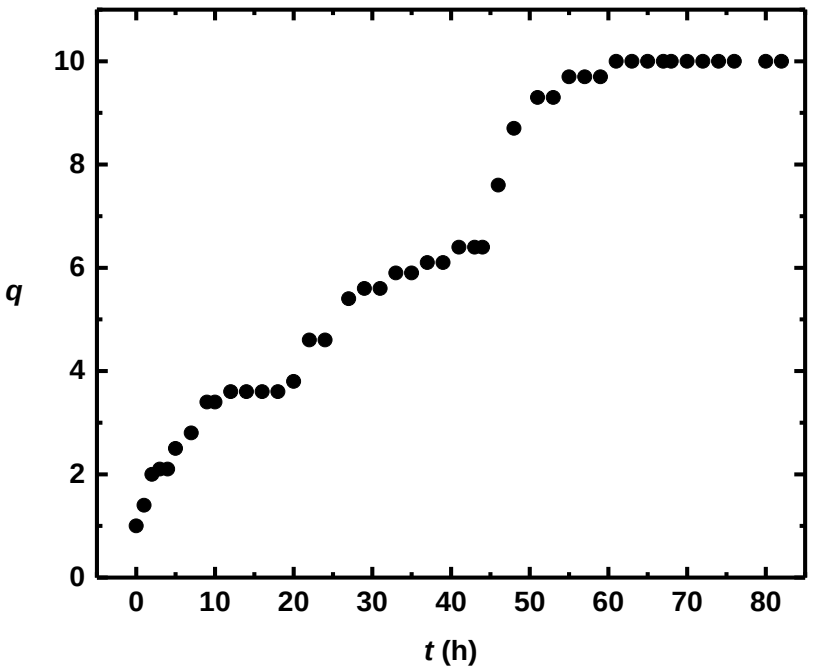

Figure S12. Swelling of a **W_2-PDCPD** xerogel in benzene with time.

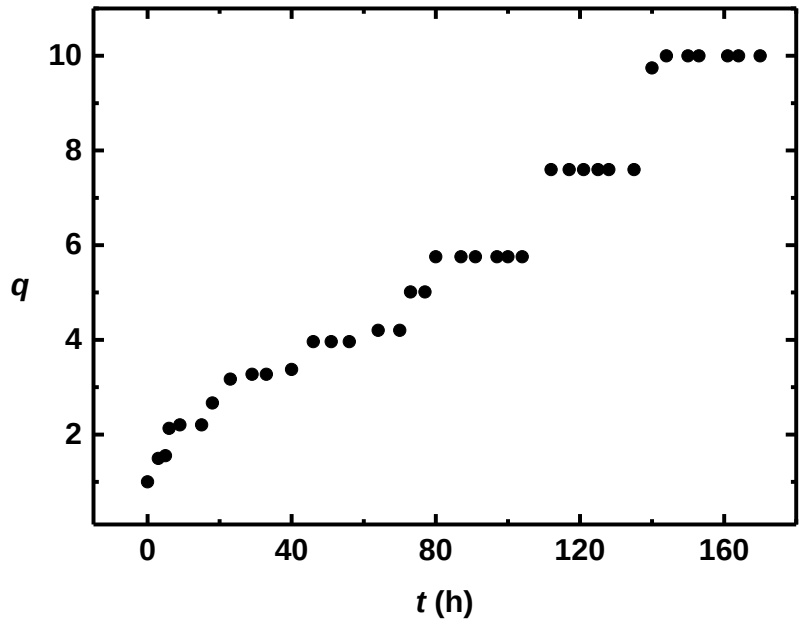

Figure S13. Swelling of a **W_2-PDCPD** xerogel in ethyl bromide with time.

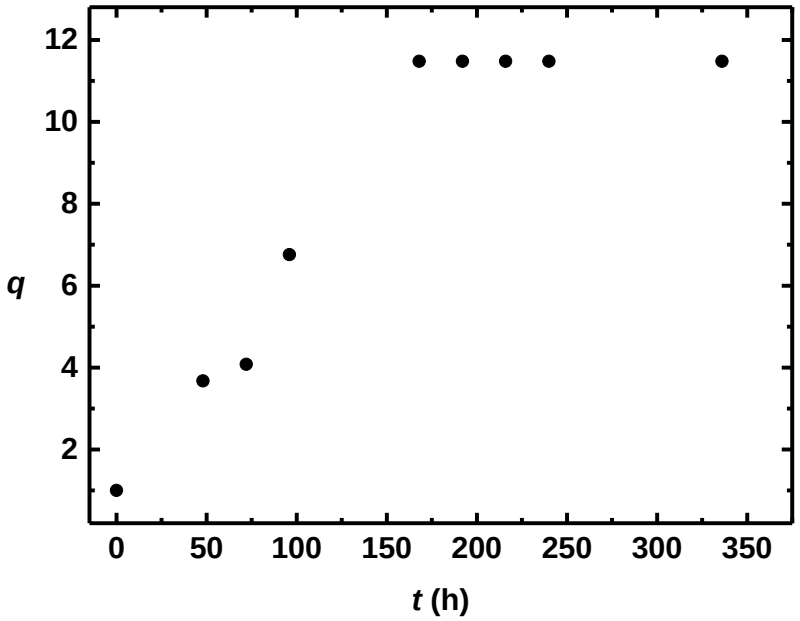

Figure S14. Swelling of a **W_2-PDCPD** xerogel in 1-bromobutane with time.

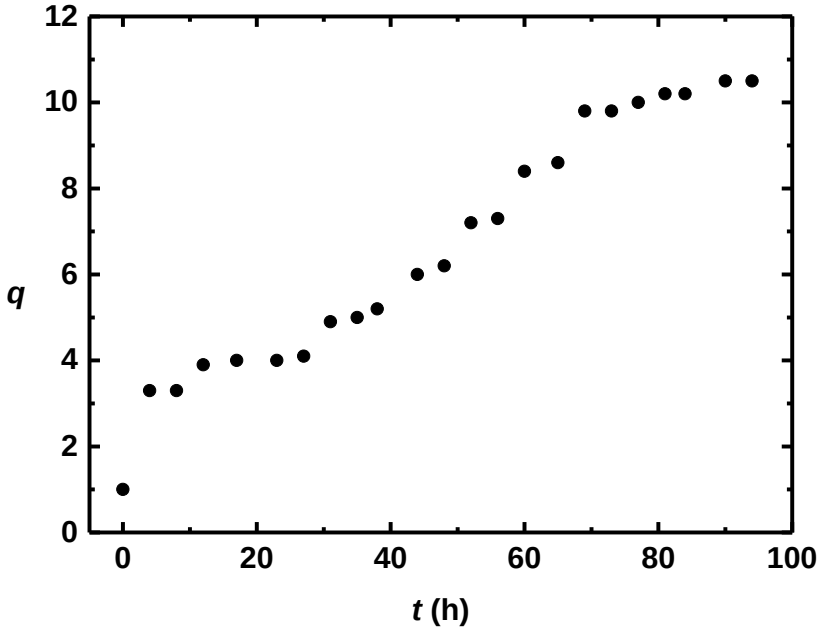

Figure S15. Swelling of a **W_2-PDCPD** xerogel in methylene dichloride with time.

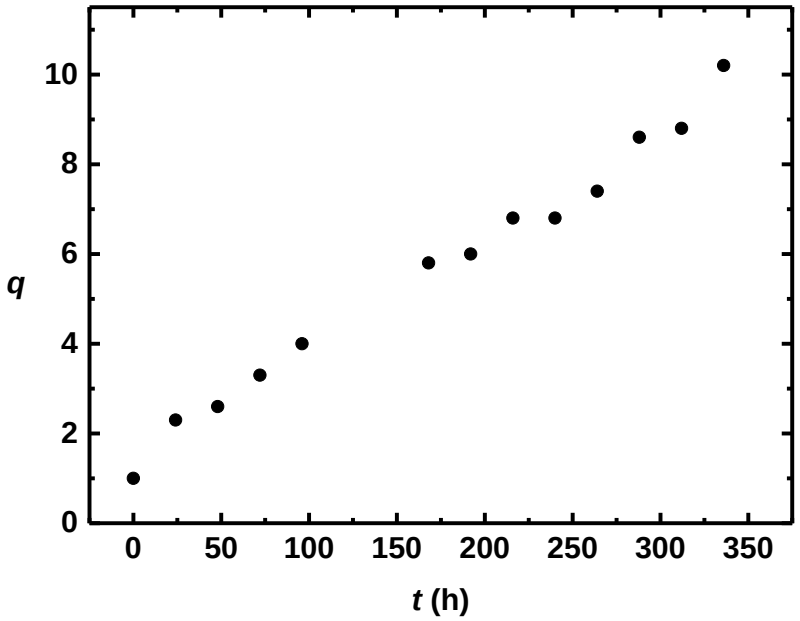

Figure S16. Swelling of a **W_2-PDCPD** xerogel in 1,3,5-trimethylbenzene with time.

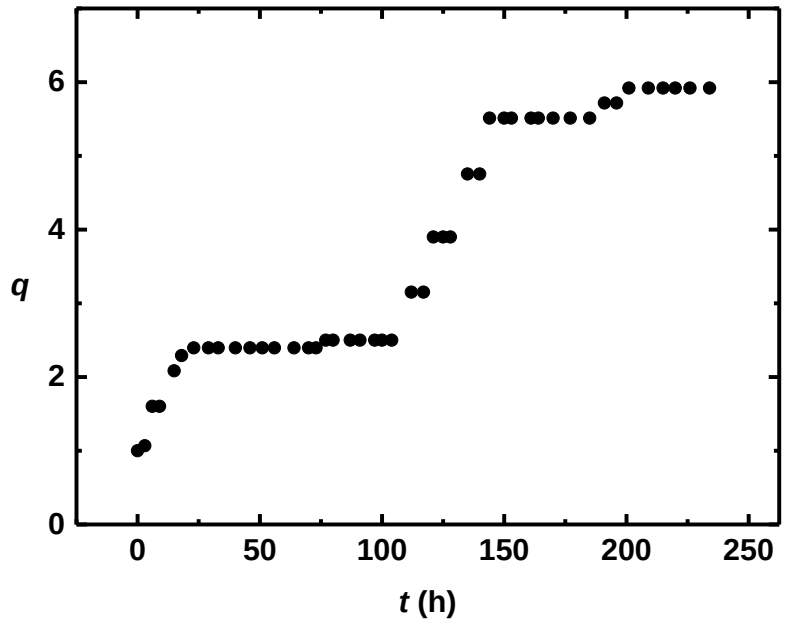

Figure S17. Swelling of a **W_2-PDCPD** xerogel in 1,4-dimethylbenzene with time.

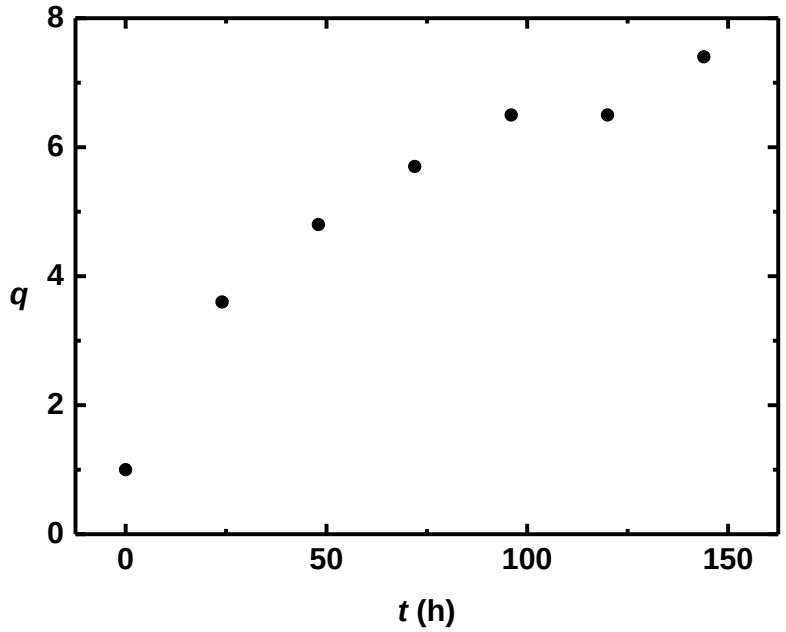

Figure S18. Swelling of a **W_2-PDCPD** xerogel in 1,3-dimethylbenzene with time.

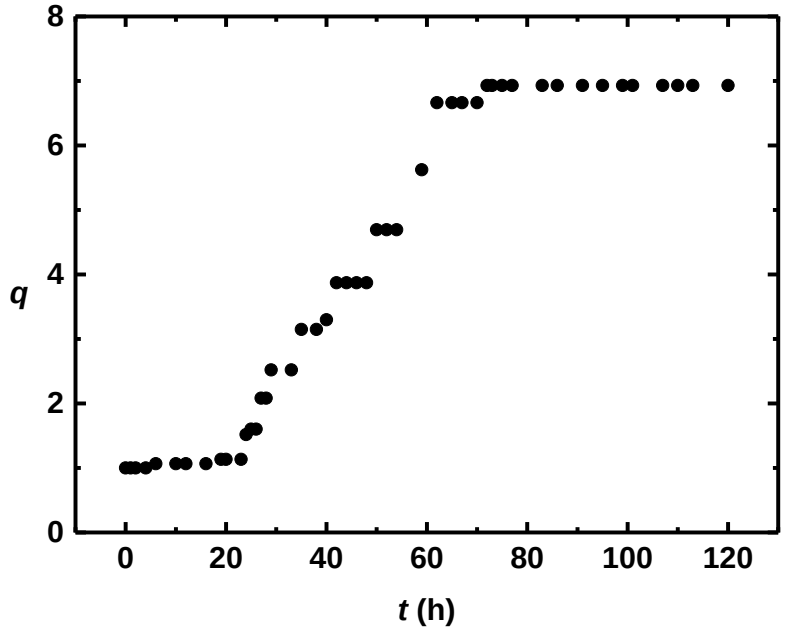

Figure S19. Swelling of a **W_2-PDCPD** xerogel in 1,2-dichlorobenzene with time.

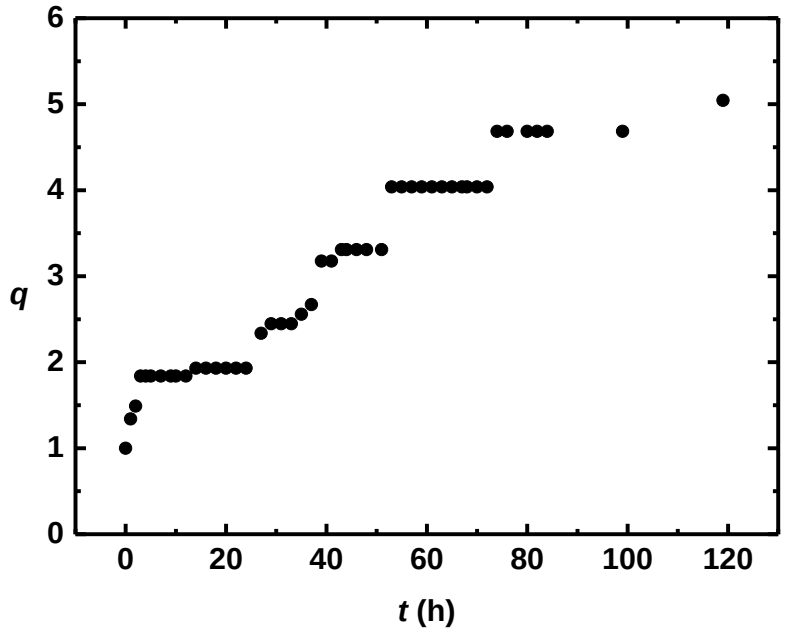

Figure S20. Swelling of a **W_2-PDCPD** xerogel in benzyl chloride with time.

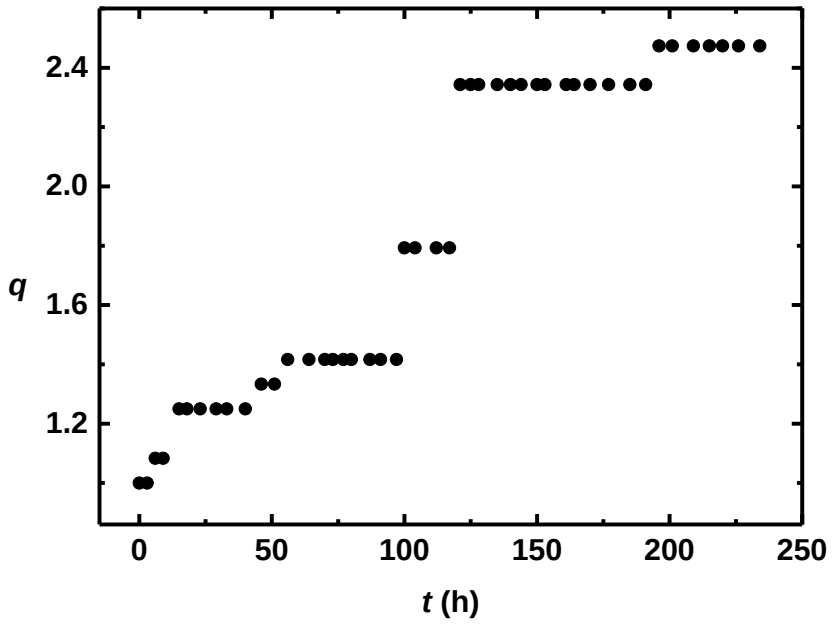

Figure S21. Swelling of a **W_2-PDCPD** xerogel in cyclohexane with time.

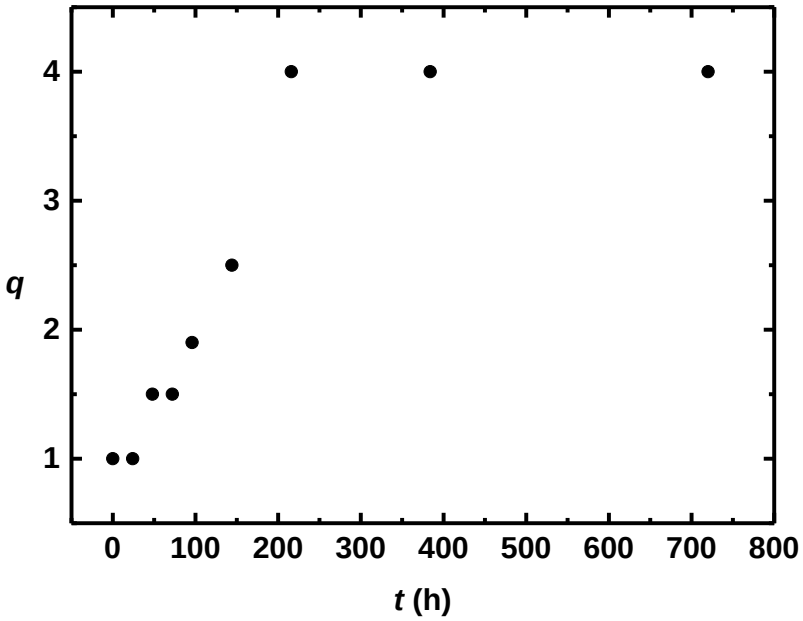

Figure S22. Swelling of a **W_2-PDCPD** xerogel in 1,4-dioxane with time.

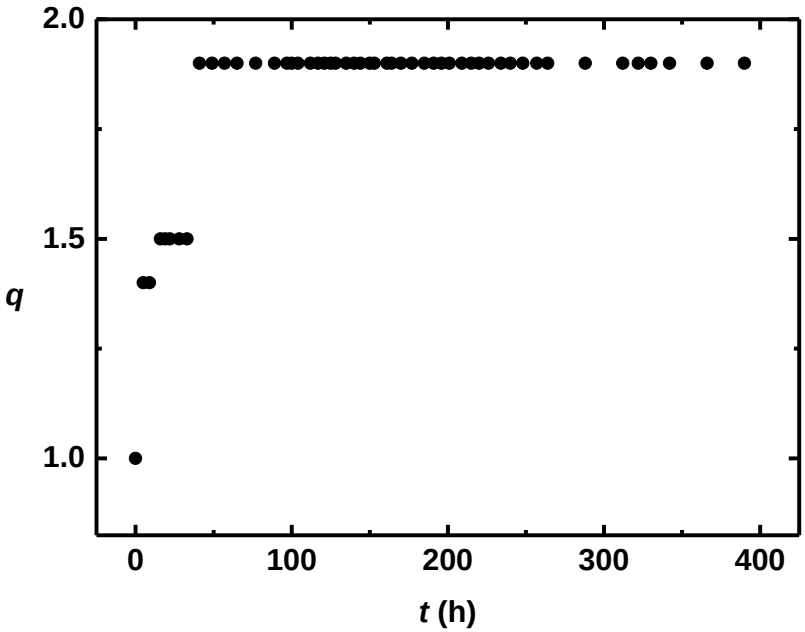

Figure S23. Swelling of a **W_2-PDCPD** xerogel in cyclohexanone with time.

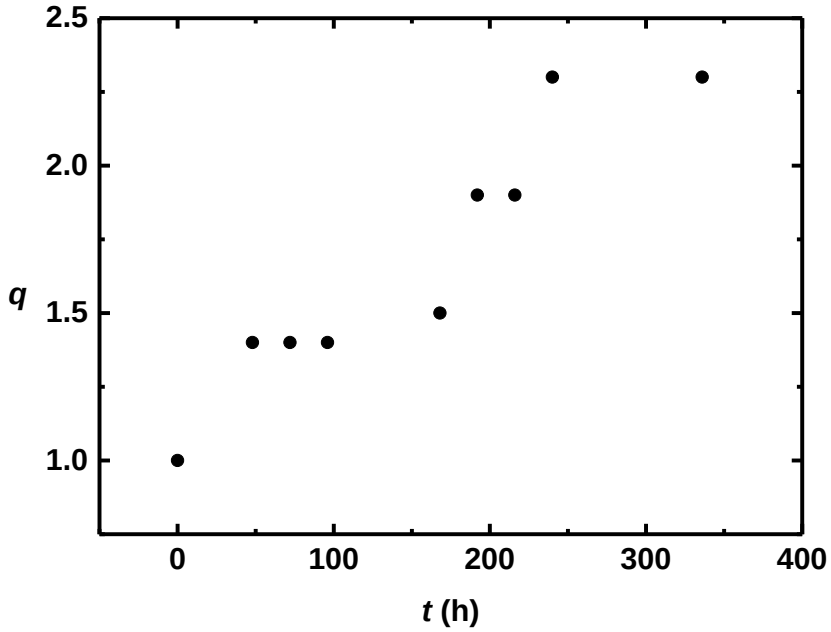

Figure S24. Swelling of a **W_2-PDCPD** xerogel in 1,2-dichloroethane with time.

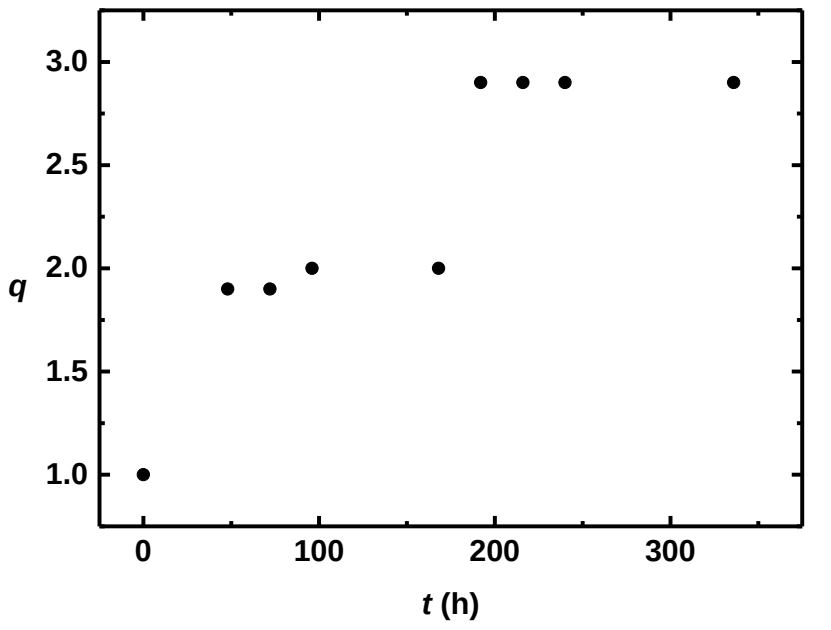

Figure S25. Swelling of a **W_2-PDCPD** xerogel in pyridine with time.

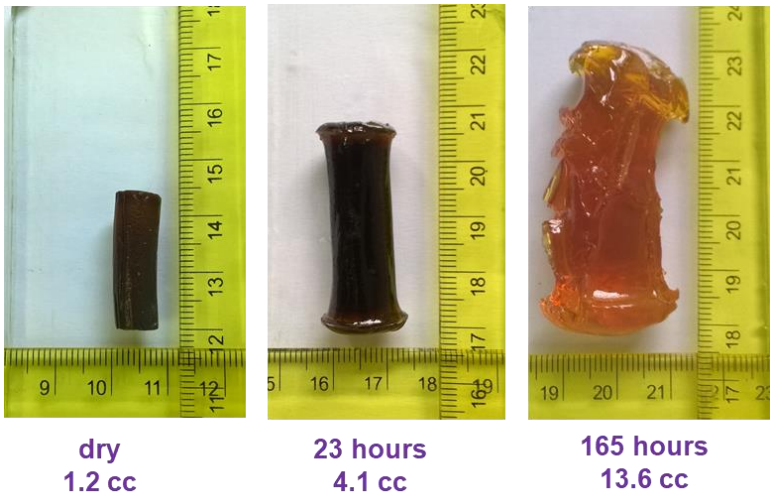

Figure S26. Swelling of a **W_2-PDCPD** xerogel in bromobenzene.

Figure S27. Swelling of a **W_2-PDCPD** xerogel in carbon disulfide.

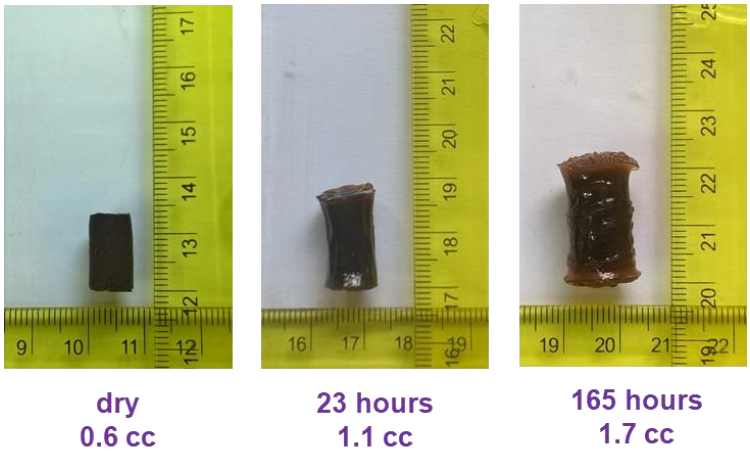

Figure S28. Swelling of a **W_2-PDCPD** xerogel in 1,2-dibromoethane.

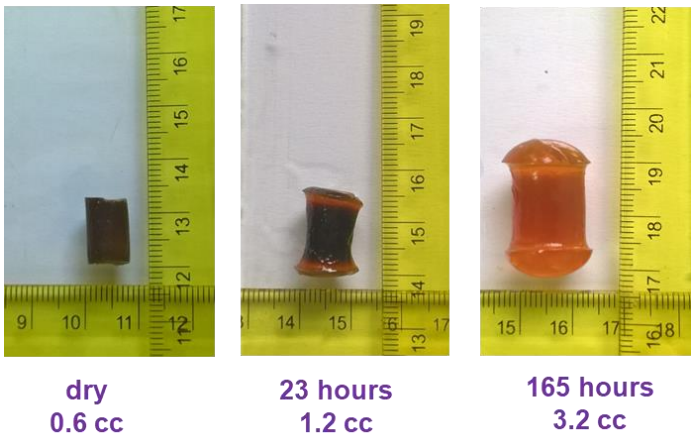

Figure S29. Swelling of a **W_2-PDCPD** xerogel in 1,3,5-trimethylbenzene.

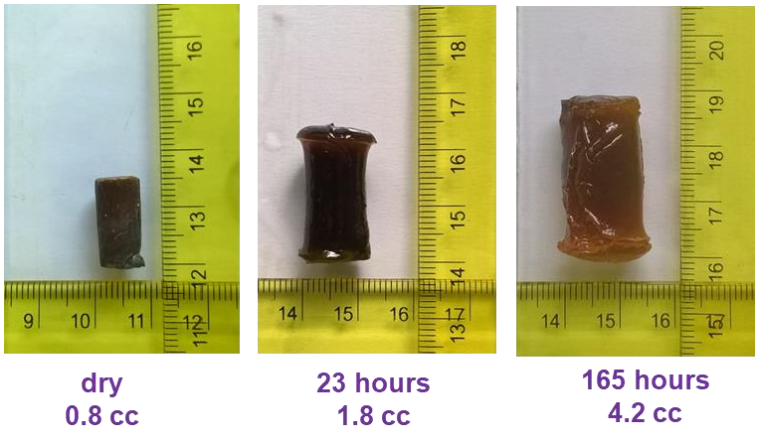

Figure S30. Swelling of a **W_2-PDCPD** xerogel in 1,4-dimethylbenzene.

Figure S31. Swelling of a **W_2-PDCPD** xerogel in 1,3-dimethylbenzene.

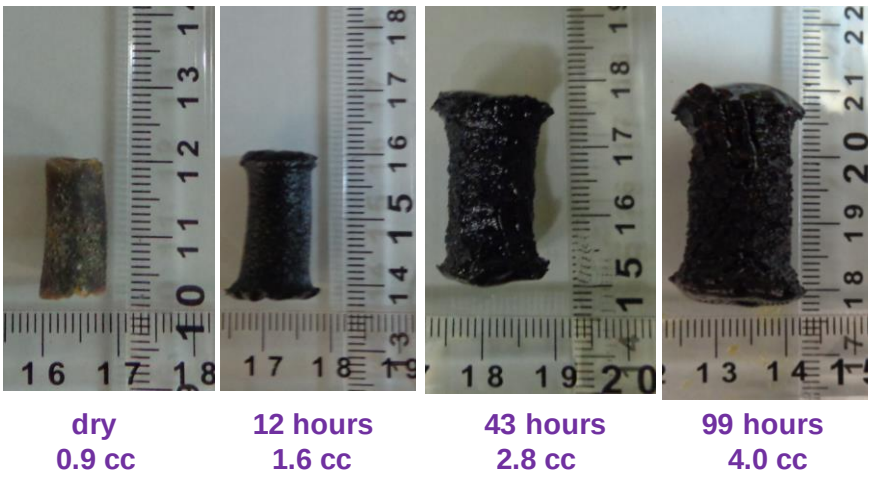

Figure S32. Swelling of a **W_2-PDCPD** xerogel in benzyl chloride.

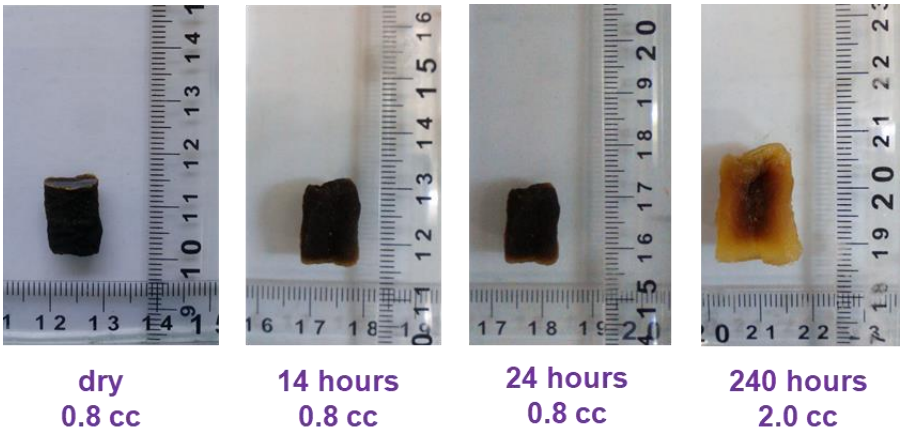

Figure S33. Swelling of a **W_2-PDCPD** xerogel in 1,4-dioxane.

Comparison of solvent uptake of W₂-PDCPD xerogels with polymeric materials from the literature

By comparison to other organic polymers on per weight basis, **W₂-PDCPD** xerogels showed higher solvent uptake for toluene and $CHCl_3$ in several cases. Specifically, they outperformed: (a) photoresponsive copolymers derived from isodecyl acrylate, lauryl acrylate, *tert*-butylstyrene and 4-(methacrylamino)azobenzene (~7× higher for toluene and ~4× higher for $CHCl_3$);[1] (b) copolymers of cinnamoyloxy ethyl methacrylate and octadecyl acrylate (~3× higher for toluene);[2] (c) disulfide-linked polymeric networks based on trimethylolpropane tris(3-mercaptopropionate), or on pentaerythritol tetrakis(3-mercaptopropionate) (more than 80× higher for $CHCl_3$ and ~6× higher for CH_2Cl_2);[3] (d) mesogenic polyelectrolyte gels (~13× higher for $CHCl_3$);[4] (e) conjugated microporous (co)polymers synthesized from 1,3,5-triethynylbenzene or 1,3,5-triethynylbenzene and 1,4-diethynylbenzene (~5× higher for $CHCl_3$);[5] (f) polymethylsilsesquioxanes (appr. 6× higher for $CHCl_3$);[6] (g) porous polyurea monoliths derived from toluene diisocyanate (~11× higher for toluene, ~6× higher for $CHCl_3$);[7] (h) *cis*-9-octadecenyl-based polymers (~30× higher for toluene, ~10× higher for $CHCl_3$, ~2× higher for THF, ~2.5× higher for CH_2Cl_2, ~3× higher for benzene);[8] and (i) poly(alkoxysilanes) (more than 11× higher for toluene, ~1.5× higher for benzene, almost equal for THF and CH_2Cl_2).[9] On the other hand, solvent uptake was equal to or lower than what was reported for the photoresponsive polymer mentioned above (almost equal for CH_2Cl_2),[1] nanoporous polydivinylbenzene (almost equal for benzene),[10] mesogenic polyelectrolyte gels (~4× lower for THF and ~7× lower for CH_2Cl_2),[4] and melamine formaldehyde sponges (~2× lower for $CHCl_3$).[11] The last three materials as well as polymethylsilsesquioxanes could also absorb solvents that **W₂-PDCPD** did not absorb (e.g., DMF, DMSO, ketones, alcohols, alkanes).[4,6,11] Compared to crosslinked lipophilic polyelectrolytes, **W₂-PDCPD** showed higher uptake of toluene (~7×), almost equal uptake of $CHCl_3$, and lower uptakes of chlorobenzene (~2×), THF (~8×), CH_2Cl_2 (~8×), dichloroethane (~65×), while those materials could also absorb several solvents that could not be absorbed by **W₂-PDCPD** xerogels, mainly alcohols and ketones, signifying the superiority of the latter in terms of selectivity.[12]

Table S1. Solvent uptake and density of **W_2-PDCPD** xerogels and other materials from the literature, for comparison purposes.

Material	Bulk density (g cm^{-3})	Toluene uptake			Chloroform uptake		
		(g g^{-1})	(g cm^{-3})	(cm^3 cm^{-3})	(g g^{-1})	(g cm^{-3})	(cm^3 cm^{-3})
Polymeric materials							
W_2-PDCPD	0.9	111	100	115[13]	89	80	54[this work]
polyurethane foams[14]	0.061	28	1.7	2			
WCl_6-PDCPD[13]	0.9	4.3	3.9	4.5			
GC-II-PDCPD aerogels[15]	<1[b]			1.5			
GC-I-PDCPD[16]					3.38		
GC-I-PDCPD aerogels	0.282[15]	0	0	0[13]			
ROMP polymers from norbornene-terminated macromonomers[17]		36					
porous polyurea monoliths[7]	0.093	10.14	0.94	1.1	15.02	1.40	0.94
photoresponsive copolymer[1]	<1[b]	15			19.5		
cinnamoyloxy ethyl methacrylate/octadecyl acrylate copolymers[2]	0.54	34	18	21			
cis-9-octadecenyl-based polymers[8]		3.69			8.5		
disulfide-linked polymeric networks[3]		0.5			1.0		
conjugated microporous (co)polymers[5]	0.027				16	0.4	0.3
melamine formaldehyde sponges[11]	0.010[a]				200	2.0	1.3
mesogenic polyelectrolyte gels[4]					6.5		
crosslinked lipophilic polyelectrolytes[12]		15			75		
polymethylsilsesquioxanes[6]	0.12				15	1.8	1.2
poly(alkoxysilanes)[9]		8.92					
Carbon materials							
carbon nanotube sponges[18]	0.005-0.010				175	0.9-1.75	
graphene/carbon composite aerogels[19]	0.003	279	0.8	1.0	400	1.2	0.8
ultra-flyweight carbon aerogels[20]	0.00016	350	0.06	0.06	550	0.09	0.06
nitrogen-doped graphene[21]	0.002	200	0.4	0.5	500	1.0	0.7
spongy graphene[22]	0.012	55	0.7	0.8	85	1.0	0.7
graphene/FeOOH aerogels[23]		15					

[a] The density of melamine formaldehyde sponges has not been measured, but ref. 8 states that similar materials have densities below 0.010 g cm^{-3}. [b] Polymers were floating on water.

Table S2. Experimental maximum volume degree of swelling (q_{max}) of **W$_2$-PDCPD** xerogels in various solvents; Hansen Solubility Parameters (HSP),[24] molar volume (V_m)[24] and surface tension (γ) of the solvents used in this study.

Solvent	q_{max} [a]	δ_D (MPa$^{1/2}$)	δ_P (MPa$^{1/2}$)	δ_H (MPa$^{1/2}$)	δ_T (MPa$^{1/2}$)	V_m (cm^3/mol)	γ [b] (mN/m)
toluene	115	18.0	1.4	2.0	18.2	106.6	26.6
chloroform	54	16.8	5.7	8.0	19.5	80.5	25.3
bromobenzene	24	17.8	3.1	5.7	18.9	105.6	27.7
carbon disulfide	21	19.2	5.5	4.1	20.4	60.6	26.7
1,3-dichlorobenzene	19	20.2	0.0	0.6	20.2	114.5	33.9
carbon tetrachloride	16	19.2	5.1	2.7	20.0	97.1	30.6
chlorobenzene	14	19.0	4.3	2.0	19.6	102.1	30.0
1,2-dibromoethane	13	19.2	3.5	8.6	21.3	86.6	32.0
tetrahydrofuran	12	17.8	0.0	0.6	17.8	81.9	23.5
benzene	12	17.0	7.3	7.1	19.8	89.5	27.1
ethyl bromide	12	18.4	0.0	2.0	18.5	74.6	24.5
1-bromobutane	11	16.5	8.4	2.3	18.7	100.0	25.4
methylene dichloride	10	16.5	3.6	3.0	17.2	64.4	19.6
1,3,5-trimethylbenzene	8	18.0	0.6	0.6	18.0	139.5	28.8
1,4-dimethylbenzene	7	17.8	1.0	3.1	18.1	121.1	27.4
1,3-dimethylbenzene	7	18.0	2.3	2.3	18.3	100.0	26.2
1,2-dichlorobenzene	7	19.2	6.3	3.3	20.5	148.5	36.3
benzyl chloride	5	16.8	0.0	0.2	16.8	115.4	23.5
cyclohexane	4	18.8	7.1	2.6	20.3	108.9	31.8
1,4-dioxane	4	17.5	1.8	9.0	19.8	85.7	27.1
cyclohexanone	2	17.8	8.4	5.1	20.3	104.2	30.4
1,2-dichloroethane	2	17.0	7.3	7.1	19.8	148.5	32.1
pyridine	2	19.0	8.8	5.9	21.8	80.9	31.9
water	1	15.5	16.0	42.3	47.8	18.0	68.7
pentane	1	14.5	0.0	0.0	14.5	116.0	17.5
N,N-dimethylformamide	1	17.4	13.7	11.3	24.9	77.4	36.6
methanol	1	14.7	12.3	22.3	29.4	40.6	- [c]
dimethylsulfoxide	1	18.4	16.4	10.2	26.7	71.3	40.7
diethyl ether	1	14.5	2.9	4.6	15.5	104.7	18.4
acetonitrile	1	15.3	18.0	6.1	24.4	52.9	29.7
acetone	1	15.5	10.4	7.0	19.9	73.8	24.3
hexane	1	14.9	0.0	0.0	14.9	131.4	19.3
2-propanol	1	15.8	6.1	16.4	23.6	76.9	- [c]
glycerol	1	17.4	11.3	27.2	34.2	73.4	- [c]
ethylene glycol	1	17.0	11.0	26.0	33.0	55.9	- [c]
benzyl alcohol	1	18.4	6.3	13.7	23.8	103.8	38.7
N,N-dimethylacetamide	1	16.8	11.5	9.4	22.4	93.0	32.6
methyl-2-pyrrolidone	1	18.0	12.3	7.2	23.0	96.6	35.5
triethylamine	1	15.5	0.4	1.0	15.5	139.7	21.4
diisopropylamine	1	14.8	3.7	1.5	15.3	141.9	20.4
aniline	1	20.1	5.8	11.2	23.7	91.6	38.9
methyl methacrylate	1	15.8	6.5	5.4	17.9	106.7	23.9
propylene carbonate	1	20.0	18.0	4.1	27.2	85.2	46.3
ethyl acetate	1	15.8	5.3	7.2	18.2	98.6	23.7

[a] Experimental maximum volume degree of swelling of **W$_2$-PDCPD** gels at t_{max} (mean values of at least three measurements), calculated according to the equation $q_{max} = V_{max}/V_{in}$, where V_{max} is the volume of the wet-gel at t_{max} and V_{in} is the initial volume of the xerogel. [b] Surface tension (γ) calculated from Beerbower's equation: $\gamma = 0.01709\ V_m^{1/3}\ [\delta_D^2 + 0.632(\delta_P^2 + \delta_H^2)]$. [c] Beerbower's equation is not valid for aliphatic alcohols.

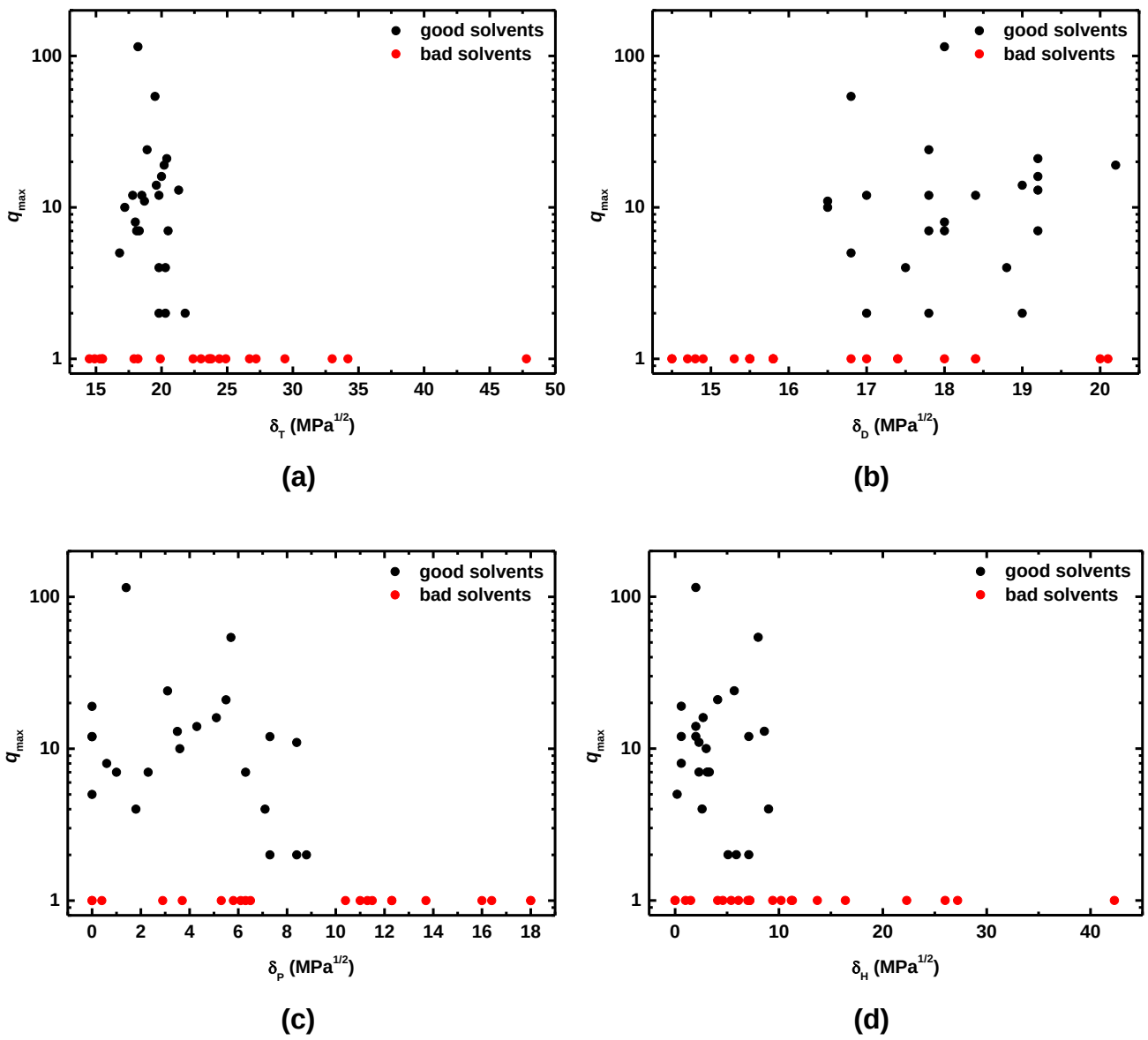

Figure S34. Relation between the experimental maximum volume degree of swelling (q_{max}) of **W$_2$-PDCPD** xerogels and the Hansen Solubility Parameters (HSP): total solubility parameter (δ_T, a), D-component (δ_D, b), P-component (δ_P, c) and H-component (δ_H, d) of the respective solvents.

1st Method of HSPiP: Inside-Out Solvents

Table S3 shows the HSP of all solvents used in this study, their empirical classification as score "1" solvents (gels swelled) or score "0" solvents (gels did not swell) and the corresponding RED (Relative Energy Difference) values. RED values were calculated using the formula: RED = (distance of solvent from the center of the sphere) / (radius of the sphere). RED values close to 0 indicate higher, and RED values close to 1 indicate lower affinity of the solvent with the molecule under study (located at the center of the sphere).

Figure S35 shows the generated sphere (R = 5.9) and the HSP (in $MPa^{1/2}$) for **W_2-PDCPD**: δ_D = 18.15, δ_P = 3.69, δ_H = 3.55 $MPa^{1/2}$, and δ_T = 18.86 $MPa^{1/2}$. The 2D plots (Figure S36) display the boundaries in HSP space and help visualize whether the solvents tested cover sufficiently the entire range of each solubility parameter (δ_P, δ_D, and δ_H). It is obvious that solvents covering the entire range of the three HSPs have been used.

Table S3. Experimental maximum volume degree of swelling (q_{max}) of **W$_2$-PDCPD** xerogels in various solvents, Hansen Solubility Parameters (HSP) of the solvents,[24] scoring according to whether they are "good" ("1") or "bad" ("0") solvents, and calculated Relative Energy Differences (RED).

Solvents	q_{max} [a]	δ_D (MPa$^{1/2}$)	δ_P (MPa$^{1/2}$)	δ_H (MPa$^{1/2}$)	score	RED [b]
1,3-dimethylbenzene	115	18.0	2.3	2.3	1	0.327
chloroform	54	17.8	3.1	5.7	1	0.389
chlorobenzene	24	19.0	4.3	2.0	1	0.411
1,3-dichlorobenzene	21	19.2	5.1	2.7	1	0.470
toluene	19	18.0	1.4	2.0	1	0.485
bromobenzene	16	19.2	5.5	4.1	1	0.491
1,4-dimethylbenzene	14	17.8	1.0	3.1	1	0.502
1-bromobutane	13	16.5	8.4	2.3	1	0.577
1,2-dichlorobenzene	12	19.2	6.3	3.3	1	0.590
1,2-dichloroethane	12	17.0	7.3	7.1	1	0.624
benzyl chloride	12	18.8	7.1	2.6	1	0.665
benzene	11	18.4	0.0	2.0	1	0.683
1,3,5-trimethylbenzene	10	18.0	0.6	0.6	1	0.781
carbon tetrachloride	8	17.8	0.0	0.6	1	0.820
cyclohexanone	7	17.8	8.4	5.1	1	0.869
methylene dichloride	7	1.7	7.3	7.1	1	0.891
1,2-dibromoethane	7	19.2	3.5	8.6	1	0.922
tetrahydrofuran	5	16.8	5.7	8.0	1	0.931
ethyl bromide	4	18.4	0.0	2.0	1	0.966
pyridine	4	19.0	8.8	5.9	1	0.977
carbon disulfide	2	20.2	0.0	0.6	1	0.992
cyclohexane	2	16.8	0.0	0.2	1	0.992
1,4-dioxane	2	17.5	1.8	9.0	1	0.994
methyl methacrylate	1	15.8	6.5	5.4	0	1.007
ethyl acetate	1	15.8	5.3	7.2	0	1.061
trimethylamine	1	15.5	0.4	1.0	0	1.229
diisopropylamine	1	14.8	3.7	1.5	0	1.278
diethyl ether	1	14.5	2.9	4.6	0	1.289
hexane	1	14.9	0.0	0.0	0	1.493
aniline	1	20.1	5.8	11.2	0	1.503
acetone	1	15.5	10.4	7.0	0	1.511
pentane	1	14.5	0.0	0.0	0	1.576
methyl-2-pyrrolidone	1	18.0	12.3	7.2	0	1.603
N,N-dimethyl acetamide	1	16.8	11.5	9.4	0	1.724
benzyl alcohol	1	18.4	6.3	13.7	0	1.821
dimethyl formamide	1	17.4	13.7	11.3	0	2.106
2-propanol	1	15.8	6.1	16.4	0	2.293
dimethyl sulfoxide	1	18.4	16.4	10.2	0	2.339
acetonitrile	1	15.3	18.0	6.1	0	2.421
propylene carbonate	1	20.0	18.0	4.1	0	2.482
methanol	1	14.7	12.3	22.3	0	3.228
ethylene glycol	1	17.0	11.0	26.0	0	3.713
glycerol	1	17.4	11.3	27.2	0	4.076
water	1	15.5	16.0	42.3	0	5.314

[a] Experimental maximum volume degree of swelling of **W$_2$-PDCPD** gels at t_{max} (mean values of at least three measurements), calculated according to the equation $q_{max} = V_{max}/V_{in}$, where V_{max} is the volume of the wet-gel at t_{max} and V_{in} is the initial volume of the xerogel. [b] Values calculated by the HSPiP 5.1.02 software.

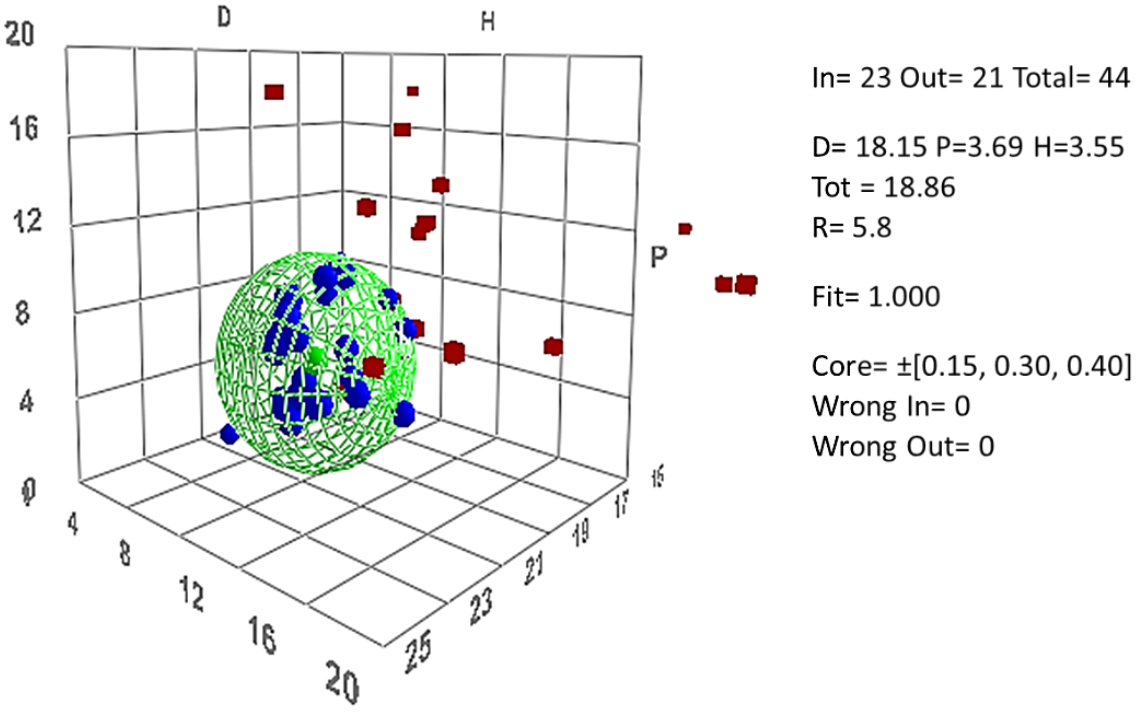

Figure S35. 3D plot of the individual Hansen Solubility Parameters (HSP) for each solvent tested. Blue dots represent solvents in which **W_2-PDCPD** xerogels swelled (23 "good" solvents – score: "1"). Red squares represent solvents in which no swelling was observed (21 "bad" solvents – score: "0"). The green sphere, generated by the HSPiP 5.1.02 software, is the sphere with the minimum diameter that fits best the experimental data. The center of the sphere is a reasonable estimate of the HSP of **W_2-PDCPD**, which is represented by the green dot. The sphere contains all "good" solvents and no "bad" solvents (referred to as wrong solvents), giving a fit value of 1.0, which is considered as a perfect fit.

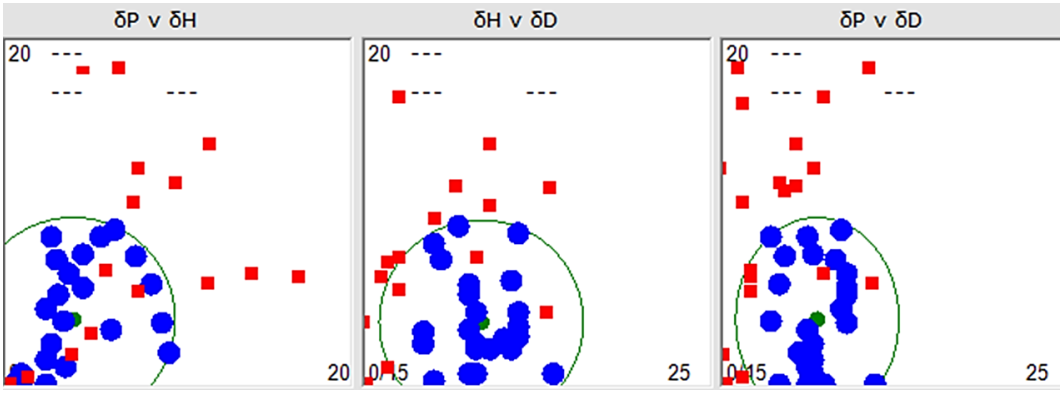

Figure S36. 2D projections, generated by the HSPiP 5.1.02 software, of the individual Hansen Solubility Parameters (HSP) for each solvent tested at the three planes of the cube inscribing the sphere of Figure S35, as indicated. Blue dots represent solvents in which **W_2-PDCPD** xerogels swelled ("good" solvents). Red squares represent solvents in which no swelling was observed ("bad" solvents). The green dot represents **W_2-PDCPD** itself. The green circle contains all "good" solvents.

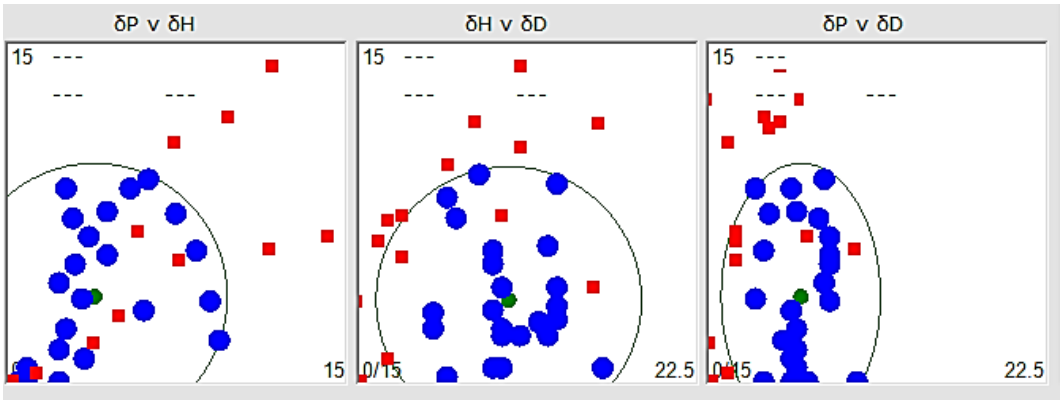

Figure S37. 2D projections, generated by the HSPiP 5.1.02 software, of the individual Hansen Solubility Parameters (HSP) for each solvent tested at the three planes of the cube inscribing the sphere of Figure 5 of the manuscript, as indicated. Blue dots represent solvents in which **W_2-PDCPD** xerogels swelled ("good" solvents). Red squares represent solvents in which no swelling was observed ("bad" solvents). The green dot represents **W_2-PDCPD** itself. The green circle contains all "good" solvents.

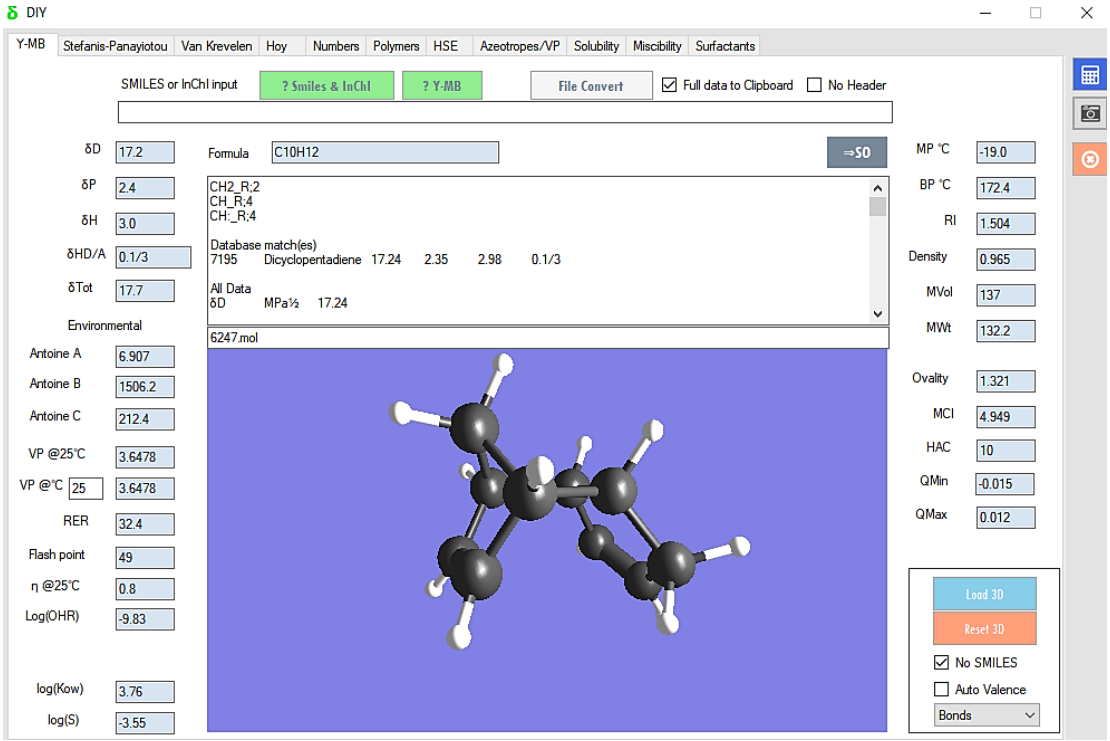

Figure S38. Calculation of the Hansen Solubility Parameters (HSP) of dicyclopentadiene (DCPD) using the DIY method of the HSPiP 5.1.02 software.

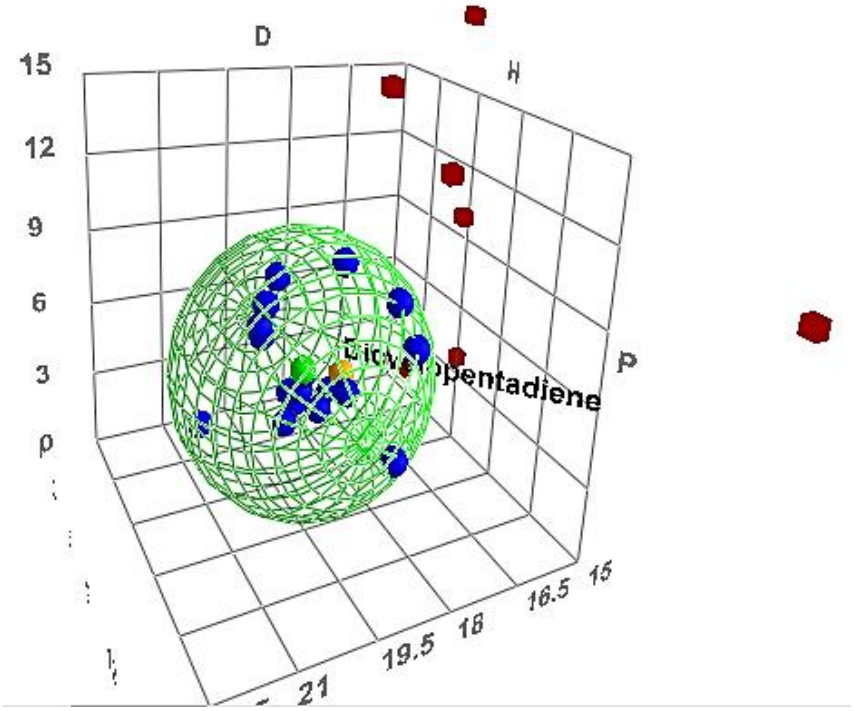

Figure S39. Same as Figure 5 of the manuscript, showing also the location of dicyclopentadiene (DCPD; orange dot; RED = 0.438).

Table S4. Calculated Hansen Solubility Parameters (HSP) of **W_2-PDCPD** xerogels and solvents.

Solvent	$\Delta 2\delta_D$ [a] ($MPa^{1/2}$)	$\Delta\delta_P$ [b] ($MPa^{1/2}$)	$\Delta\delta_H$ [c] ($MPa^{1/2}$)
toluene	0.3	2.3	1.6
chloroform	0.7	0.6	-2.2
bromobenzene	-2.1	-1.8	-0.6
carbon disulfide	-4.1	3.7	3.7
1,3-dichlorobenzene	-2.1	-1.4	0.9
carbon tetrachloride	0.7	3.7	3.0
chlorobenzene	-1.7	-0.6	1.6
1,2-dibromoethane	-2.1	0.2	-5.1
tetrahyfrofuran	2.7	-2.0	-4.5
benzene	-0.5	3.7	1.6
ethyl bromide	3.3	-4.7	1.3
1-bromobutane	3.3	0.1	0.6
methylene dichloride	2.3	-3.6	-3.6
1,3,5-trimethylbenzene	0.3	3.1	3.0
1,4-dimethylbenzene	0.7	2.7	0.5
1,3-dimethylbenzene	0.3	1.4	1.3
1,2-dichlorobenzene	-2.1	-2.6	0.3
benzyl chloride	-1.3	-3.4	1.0
cyclohexane	2.7	3.7	3.4
1,4-dioxane	1.3	1.9	-5.5
cyclohexanone	0.7	-4.7	-1.6
1,2-dichloroethane	2.3	-3.6	-3.6
pyridine	-1.7	-5.1	-2.4
water	5.3	-12.3	-38.8
pentane	7.3	3.7	3.6
N,N-dimethylformamide	1.5	-10.0	-7.8
methanol	6.9	-8.6	-18.8
dimethylsulfoxide	-0.5	-12.7	-6.7
diethyl ether	7.3	0.8	-1.1
acetonitrile	5.7	-14.3	-2.6
acetone	5.3	-6.7	-3.5
hexane	6.5	3.7	3.6
2-propanol	4.7	-2.4	-12.9
glycerol	1.5	-7.6	-23.7
ethylene glycol	2.3	-7.3	-22.5
benzyl alcohol	-0.5	-2.6	-10.2
N,*N*-dimethylacetamide	2.7	-7.8	-5.9
methyl-2-pyrrolidone	0.3	-8.6	-3.7
triethylamine	5.3	3.3	2.6
diisopropylamine	6.7	0.0	2.1
aniline	-3.9	-2.1	-7.7
methyl methacrylate	4.7	-2.8	-1.9
propylene carbonate	-3.7	-14.3	-0.6
ethyl acetate	4.7	-1.6	-3.7

[a] $\Delta 2\delta_D = (2\delta_{D1}) - (2\delta_{D2})$. [b] $(\Delta\delta_P) = (\delta_{P1}) - (\delta_{P2})$. [c] $(\Delta\delta_H) = (\delta_{H1}) - (\delta_{H2})$. "1" refers to **$W_2$-PDCPD** xerogels and "2" refers to the solvent. Hansen Solubility Parameters (HSP) for **W_2-PDCPD**: $\delta_D = 18.15$, $\delta_P = 3.69$, $\delta_H = 3.55$ $MPa^{1/2}$.

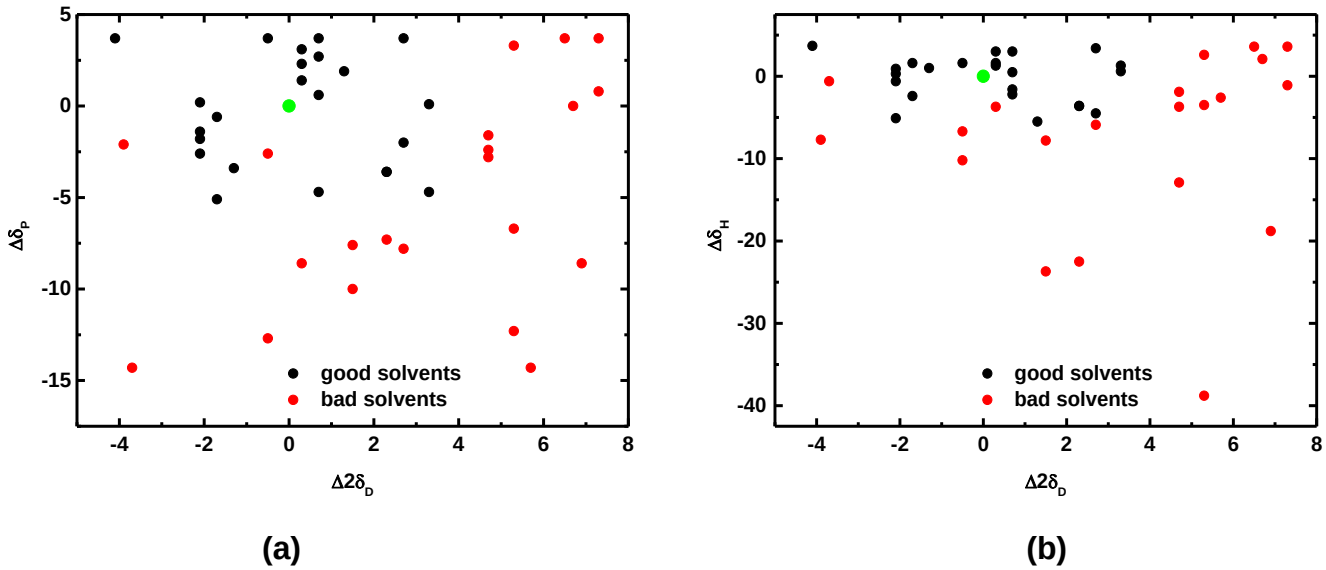

Figure S40. 2D plots of the magnitude differences between the solvent and **W$_2$-PDCPD** xerogels: $\Delta\delta_P$ *vs* $\Delta 2\delta_D$ (a) and $\Delta\delta_H$ *vs* $\Delta 2\delta_D$ (b). Green dot shows point (0,0).

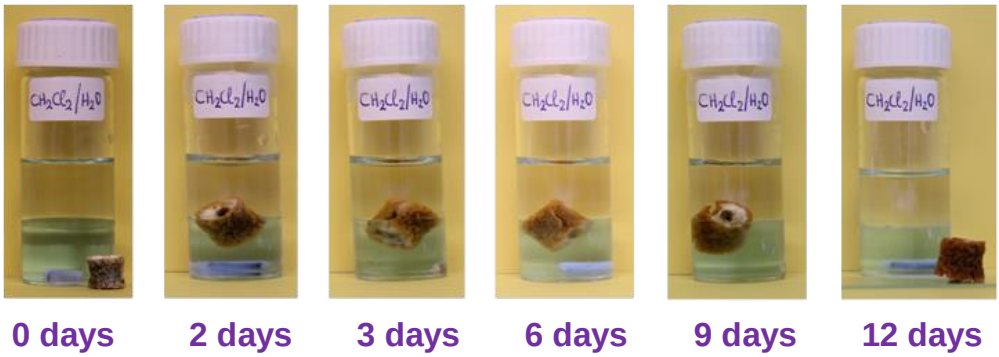

Figure S41. Separation of methylene dichloride (dyed with Sudan blue) from water using **W_2-PDCPD** xerogels.

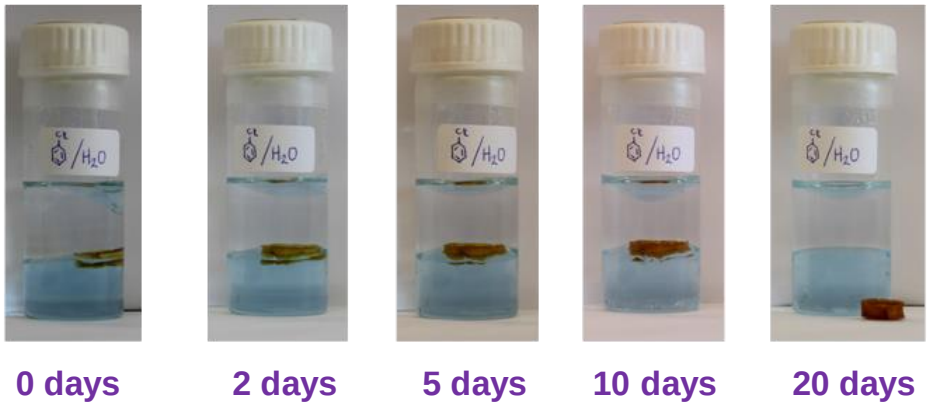

Figure S42. Separation of chlorobenzene (dyed with Sudan blue) from water using **W_2-PDCPD** xerogels.

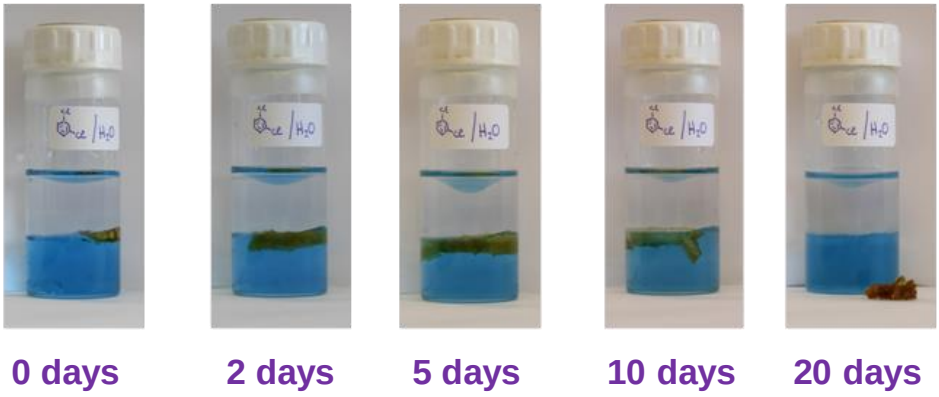

Figure S43. Separation of 1,3-dichlorobenzene (dyed with Sudan blue) from water using **W_2-PDCPD** xerogels.

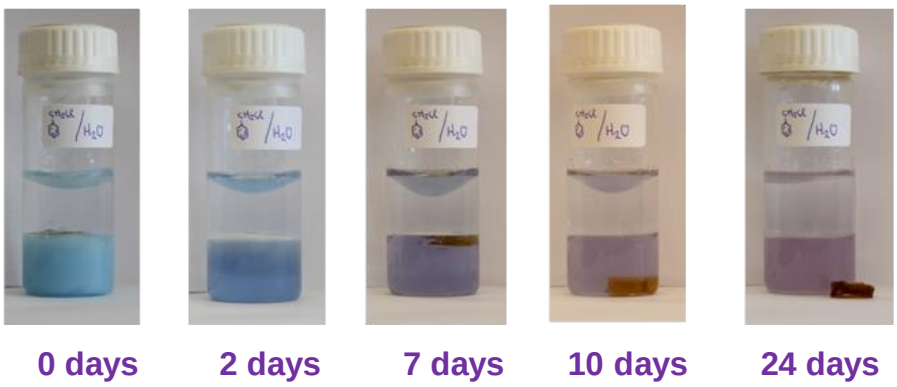

Figure S44. Separation of benzyl chloride (dyed with Sudan blue) from water using **W_2-PDCPD** xerogels.

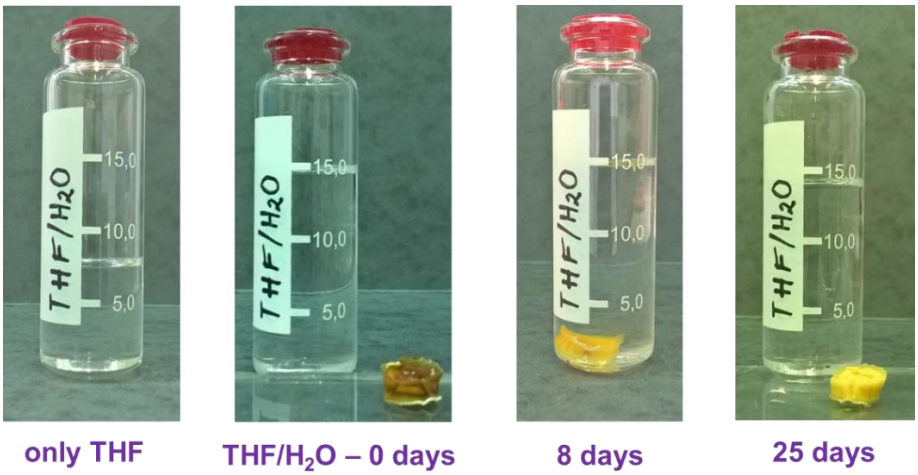

Figure S45. Separation of tetrahydrofuran from water using **W_2-PDCPD** xerogels.

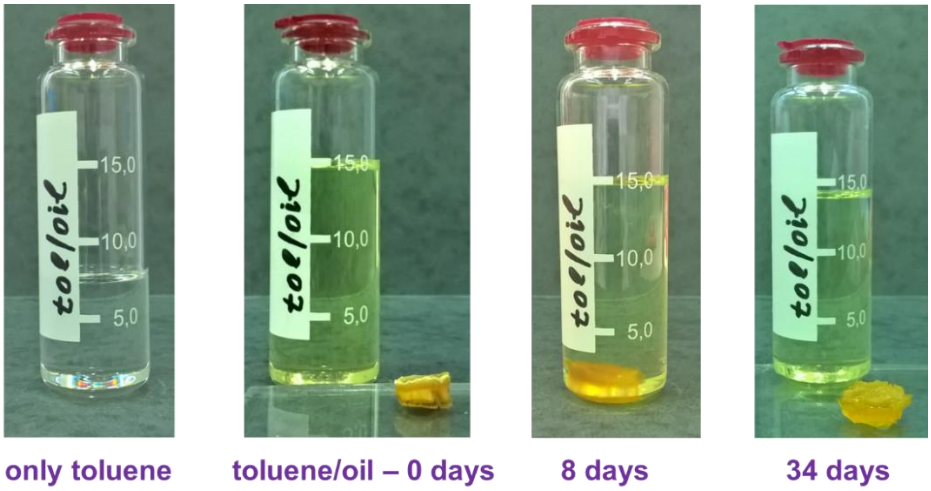

Figure S46. Separation of toluene from oil using **W_2-PDCPD** xerogels.

Figure S47. Separation of toluene from hexane using **W_2-PDCPD** xerogels.

References

(1) Kulawardana, E. U.; Neckers, D. C. Photoresponsive Oil Sorbers. *J. Polym. Sci. Part Polym. Chem.* **2010**, *48* (1), 55–62. https://doi.org/10.1002/pola.23753.

(2) Atta, A. M.; El-Ghazawy, R. A. M.; Farag, R. K.; Abdel-Azim, A.-A. A. Crosslinked Reactive Macromonomers Based on Polyisobutylene and Octadecyl Acrylate Copolymers as Crude Oil Sorbers. *React. Funct. Polym.* **2006**, *66* (9), 931–943. https://doi.org/10.1016/j.reactfunctpolym.2006.01.001.

(3) Patel, H. A.; Yavuz, M. S.; Yavuz, C. T. Exceptional Organic Solvent Uptake by Disulfide-Linked Polymeric Networks. *RSC Adv.* **2014**, *4* (46), 24320–24323. https://doi.org/10.1039/C4RA03355H.

(4) Nishikori, Y.; Iseda, K.; Kokado, K.; Sada, K.; Nishikori, Y.; Iseda, K.; Kokado, K.; Sada, K. Mesogenic Polyelectrolyte Gels Absorb Organic Solvents and Liquid Crystalline Molecules. *Polymers* **2016**, *8* (4), 148. https://doi.org/10.3390/polym8040148.

(5) Li, A.; Sun, H.-X.; Tan, D.-Z.; Fan, W.-J.; Wen, S.-H.; Qing, X.-J.; Li, G.-X.; Li, S.-Y.; Deng, W.-Q. Superhydrophobic Conjugated Microporous Polymers for Separation and Adsorption. *Energy Environ. Sci.* **2011**, *4* (6), 2062–2065. https://doi.org/10.1039/C1EE01092A.

(6) Hayase, G.; Kanamori, K.; Fukuchi, M.; Kaji, H.; Nakanishi, K. Facile Synthesis of Marshmallow-like Macroporous Gels Usable under Harsh Conditions for the Separation of Oil and Water. *Angew. Chem. Int. Ed.* **2013**, *52* (7), 1986–1989. https://doi.org/10.1002/anie.201207969.

(7) Lin, P.; Meng, L.; Huang, Y.; Liu, L. Synthesis of Porous Polyurea Monoliths Assisted by Centrifugation as Adsorbents for Water Purification. *Colloids Surf. Physicochem. Eng. Asp.* **2016**, *506*, 87–95. https://doi.org/10.1016/j.colsurfa.2016.06.017.

(8) Dutta, P.; Gogoi, B.; Dass, N. N.; Sen Sarma, N. Efficient Organic Solvent and Oil Sorbent Co-Polyesters: Poly-9-Octadecenylacrylate/Methacrylate with 1-Hexene. *React. Funct. Polym.* **2013**, *73* (3), 457–464. https://doi.org/10.1016/j.reactfunctpolym.2012.11.017.

(9) Ozan Aydin, G.; Bulbul Sonmez, H. Hydrophobic Poly(Alkoxysilane) Organogels as Sorbent Material for Oil Spill Cleanup. *Mar. Pollut. Bull.* **2015**, *96* (1), 155–164. https://doi.org/10.1016/j.marpolbul.2015.05.033.

(10) Zhang, Y.; Wei, S.; Liu, F.; Du, Y.; Liu, S.; Ji, Y.; Yokoi, T.; Tatsumi, T.; Xiao, F.-S. Superhydrophobic Nanoporous Polymers as Efficient Adsorbents for Organic Compounds. *Nano Today* **2009**, *4* (2), 135–142. https://doi.org/10.1016/j.nantod.2009.02.010.

(11) Ruan, C.; Ai, K.; Li, X.; Lu, L. A Superhydrophobic Sponge with Excellent Absorbency and Flame Retardancy. *Angew. Chem. Int. Ed.* **2014**, *53* (22), 5556–5560. https://doi.org/10.1002/anie.201400775.

(12) Ono, T.; Sugimoto, T.; Shinkai, S.; Sada, K. Molecular Design of Superabsorbent Polymers for Organic Solvents by Crosslinked Lipophilic Polyelectrolytes. *Adv. Funct. Mater.* **2008**, *18* (24), 3936–3940. https://doi.org/10.1002/adfm.200801221.

(13) Raptopoulos, G.; Anyfantis, G. C.; Chriti, D.; Paraskevopoulou, P. Synthesis and Structural Characterization of Poly(Dicyclopentadiene) Gels Obtained with a Novel Ditungsten versus Conventional W and Ru Mononuclear Catalysts. *Inorganica Chim. Acta* **2017**, *460*, 69–76. https://doi.org/10.1016/j.ica.2016.09.008.

(14) Atta, A. M.; Brostow, W.; Datashvili, T.; El-Ghazawy, R. A.; Lobland, H. E. H.; Hasan, A.-R. M.; Perez, J. M. Porous Polyurethane Foams Based on Recycled Poly(Ethylene Terephthalate) for Oil Sorption: Polyurethane Foams for Oil Sorption. *Polym. Int.* **2013**, *62* (1), 116–126. https://doi.org/10.1002/pi.4325.

(15) Bang, A.; Mohite, D.; Saeed, A. M.; Leventis, N.; Sotiriou-Leventis, C. Polydicyclopentadiene Aerogels from First- versus Second-Generation Grubbs' Catalysts: A Molecular versus a Nanoscopic Perspective. *J. Sol-Gel Sci. Technol.* **2015**, *75* (2), 460–474. https://doi.org/10.1007/s10971-015-3718-0.

(16) Long, T. R.; Gupta, A.; Ii, A. L. M.; Rethwisch, D. G.; Bowden, N. B. Selective Flux of Organic Liquids and Solids Using Nanoporous Membranes of Polydicyclopentadiene. *J. Mater. Chem.* **2011**, *21* (37), 14265–14276. https://doi.org/10.1039/C1JM10970G.

(17) Sarapas, J. M.; Chan, E. P.; Rettner, E. M.; Beers, K. L. Compressing and Swelling To Study the Structure of Extremely Soft Bottlebrush Networks Prepared by ROMP. *Macromolecules* **2018**, *51* (6), 2359–2366. https://doi.org/10.1021/acs.macromol.8b00018.

(18) Gui, X.; Wei, J.; Wang, K.; Cao, A.; Zhu, H.; Jia, Y.; Shu, Q.; Wu, D. Carbon Nanotube Sponges. *Adv. Mater.* **2010**, *22* (5), 617–621. https://doi.org/10.1002/adma.200902986.

(19) Qian, Y.; Ismail, I. M.; Stein, A. Ultralight, High-Surface-Area, Multifunctional Graphene-Based Aerogels from Self-Assembly of Graphene Oxide and Resol. *Carbon* **2014**, *68*, 221–231. https://doi.org/10.1016/j.carbon.2013.10.082.

(20) Sun, H.; Xu, Z.; Gao, C. Multifunctional, Ultra-Flyweight, Synergistically Assembled Carbon Aerogels. *Adv. Mater.* **2013**, *25* (18), 2554–2560. https://doi.org/10.1002/adma.201204576.

(21) Zhao, Y.; Hu, C.; Hu, Y.; Cheng, H.; Shi, G.; Qu, L. A Versatile, Ultralight, Nitrogen-Doped Graphene Framework. *Angew. Chem. Int. Ed.* **2012**, *51* (45), 11371–11375. https://doi.org/10.1002/anie.201206554.

(22) Bi, H.; Xie, X.; Yin, K.; Zhou, Y.; Wan, S.; He, L.; Xu, F.; Banhart, F.; Sun, L.; Ruoff, R. S. Spongy Graphene as a Highly Efficient and Recyclable Sorbent for Oils and Organic Solvents. *Adv. Funct. Mater.* **2012**, *22* (21), 4421–4425. https://doi.org/10.1002/adfm.201200888.

(23) Cong, H.-P.; Ren, X.-C.; Wang, P.; Yu, S.-H. Macroscopic Multifunctional Graphene-Based Hydrogels and Aerogels by a Metal Ion Induced Self-Assembly Process. *ACS Nano* **2012**, *6* (3), 2693–2703. https://doi.org/10.1021/nn300082k.

(24) Hansen Solubility Parameters | Hansen Solubility Parameters https://www.hansen-solubility.com/ (accessed Mar 4, 2019).